Supplementary Information

The effect of regioisomerism on the solid-state fluorescence of bis(piperidyl)anthracenes: structurally simple but bright AIE luminogens†

Shunsuke Sasaki,[a] Kazunobu Igawa,[b] and Gen-ichi Konishi*[a,c]

[a] *Department of Organic and Polymeric Materials, Tokyo Institute of Technology, Tokyo 152-8552, Japan*

[b] *Institute for Materials Chemistry and Engineering and Department of Molecular and Material Sciences, Kyushu University, Fukuoka 816-8580, Japan*

[c] *PRESTO, Japan Science and Technology Agency (JST)*

* Corresponding author; e-mail: konishi.g.aa@m.titech.ac.jp; fax: +81-3-5734-2321

S1. NMR charts

Detailed synthetic procedures and characterisation data are described in the experimental section.

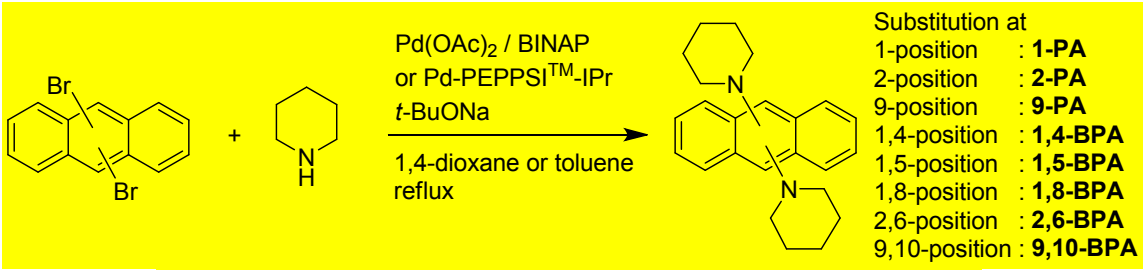

Chart S1. Synthetic route for the preparation of **PA**s and **BPA**s.

1-PA

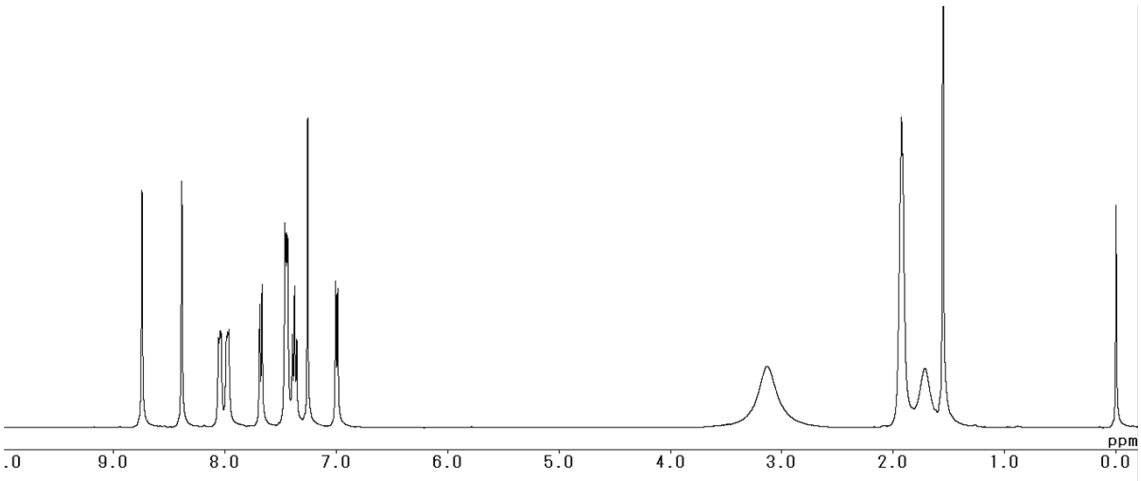

Fig. S1. ^{1}H NMR spectrum of **1-PA**, (400 MHz, $CDCl_3$).

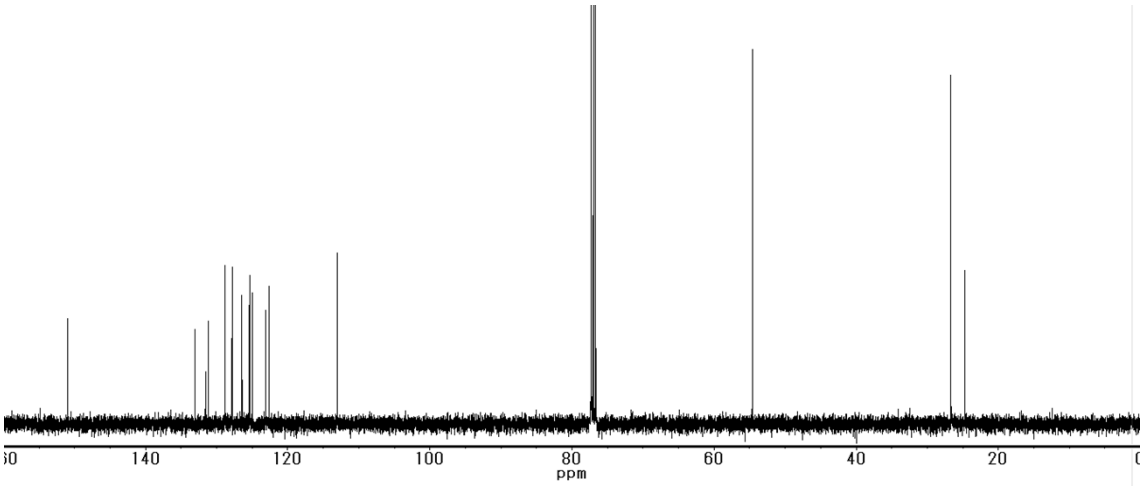

Fig. S2. ^{13}C NMR spectrum of **1-PA** (100 MHz, $CDCl_3$).

1,4-BPA

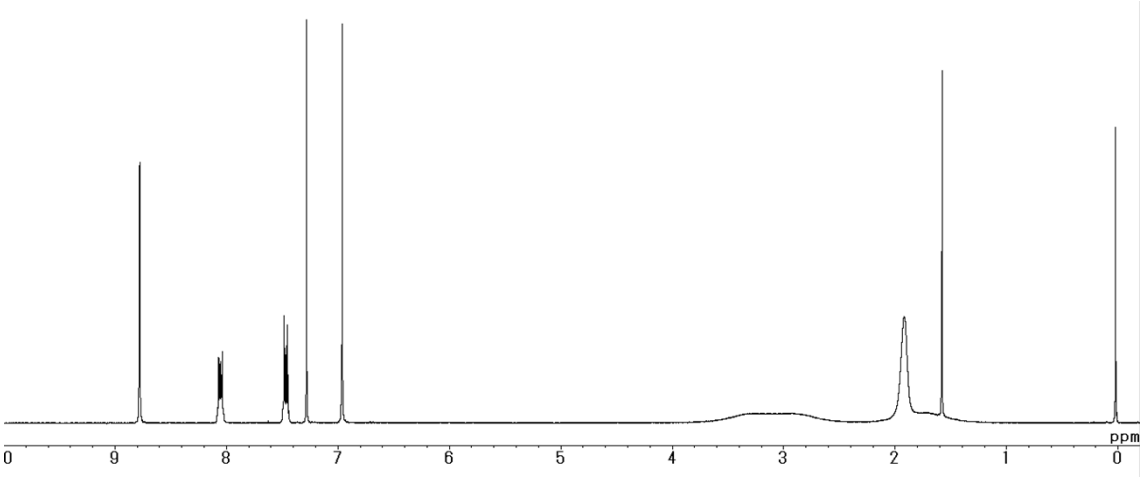

Fig. S3. ^{1}H NMR spectrum of **1,4-BPA** (300 MHz, $CDCl_3$).

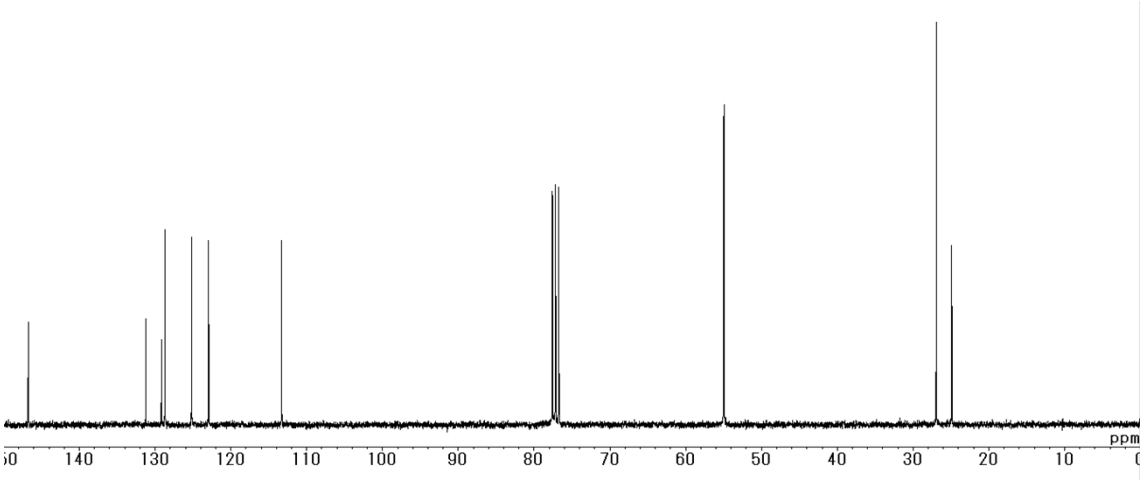

Figure S4. ^{13}C NMR spectrum of **1,4-BPA** (75 MHz, $CDCl_3$).

1,5-BPA

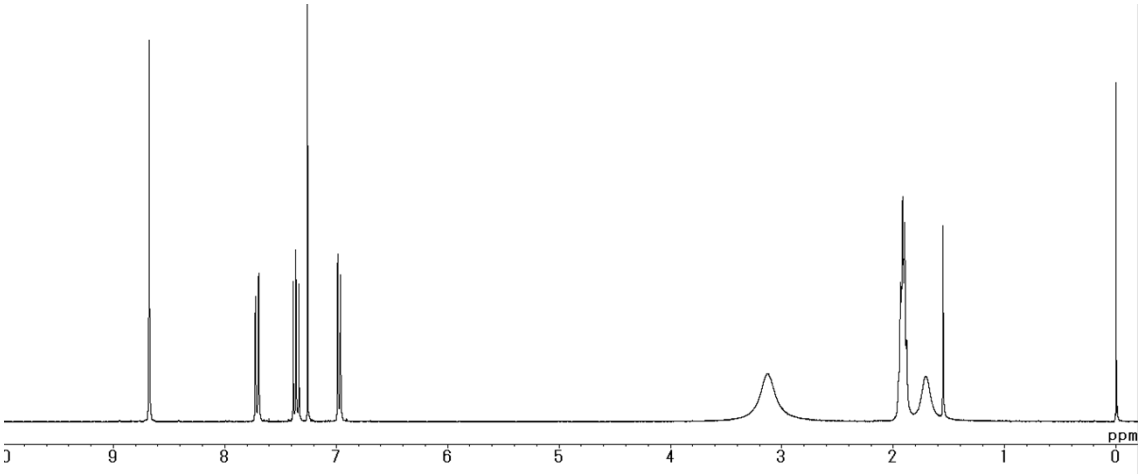

Fig. S5. ^{1}H NMR spectrum of **1,5-BPA** (300 MHz, $CDCl_3$).

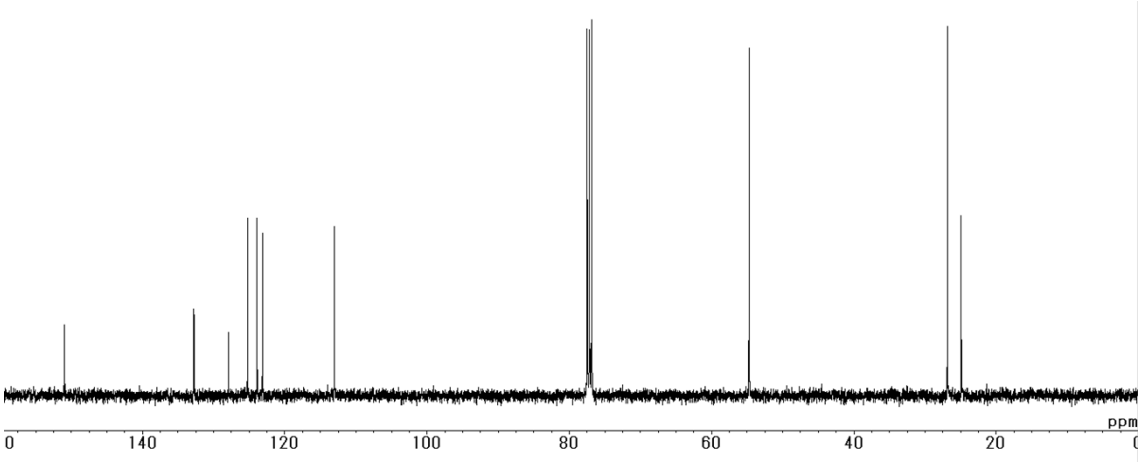

Fig. S6. ^{13}C NMR spectrum of **1,5-BPA** (100 MHz, $CDCl_3$).

1,8-BPA

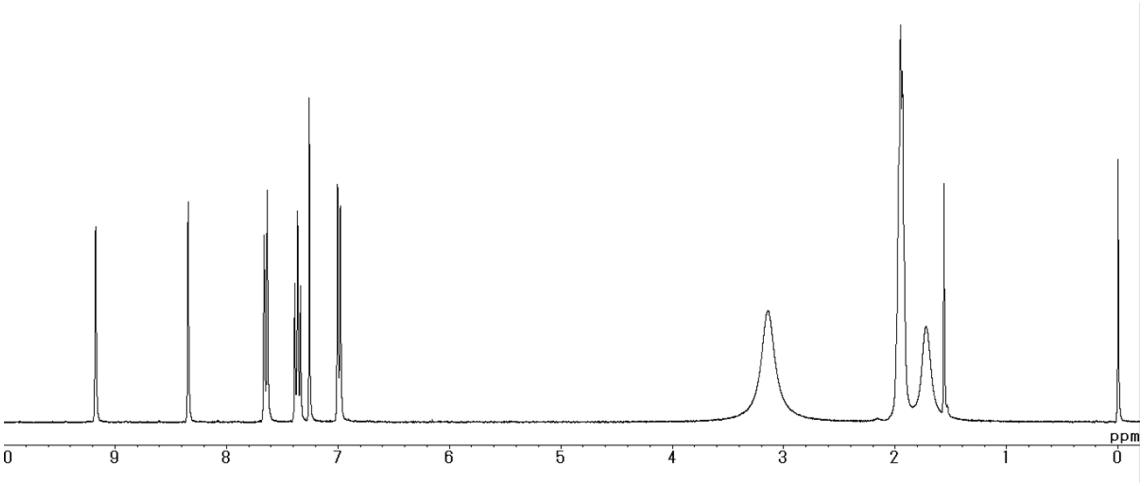

Fig. S7. ^{1}H NMR spectrum of **1,8-BPA** (300 MHz, $CDCl_3$).

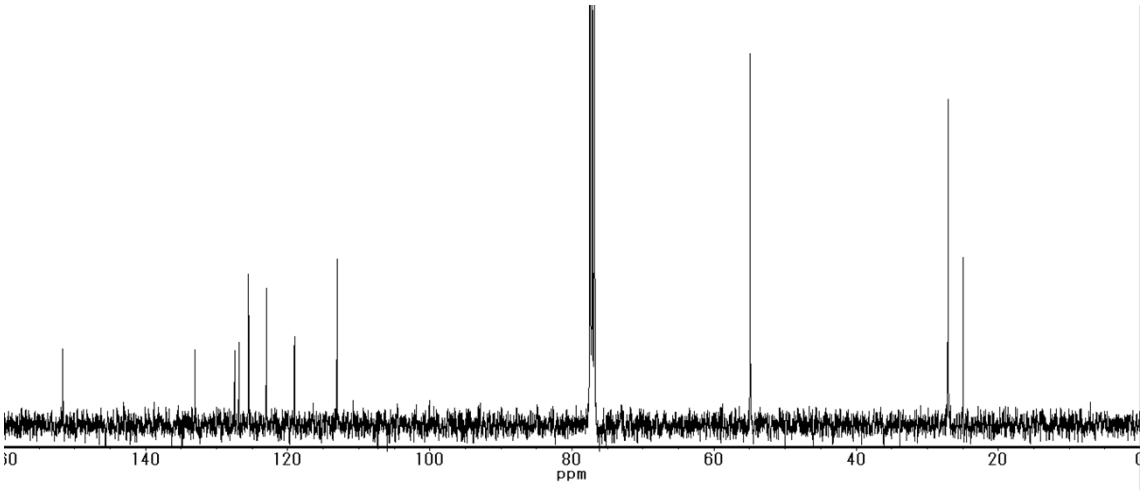

Fig. S8. ^{13}C NMR spectrum of **1,8-BPA** (100 MHz, $CDCl_3$).

2-PA

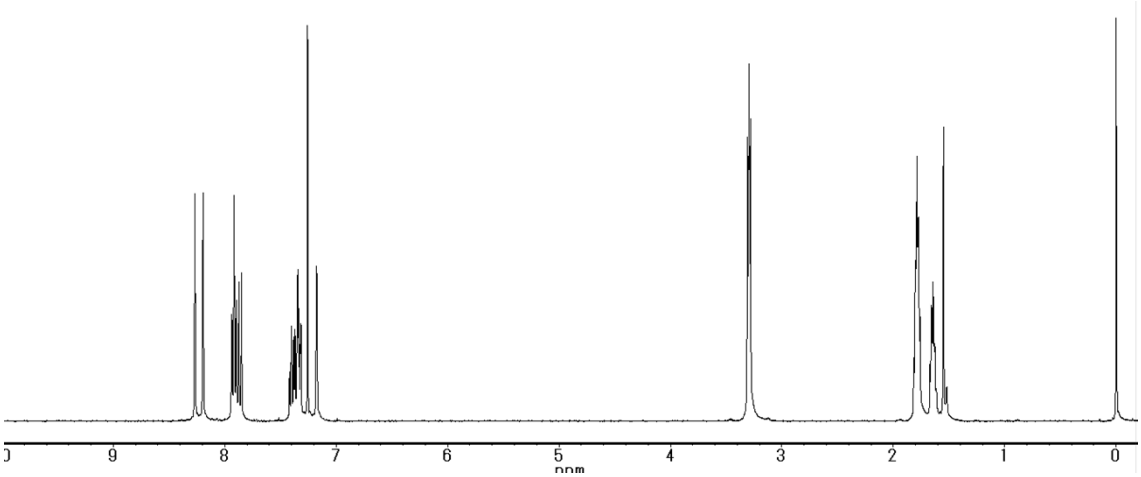

Fig. S9. ^{1}H NMR spectrum of **2-PA** (400 MHz, $CDCl_3$).

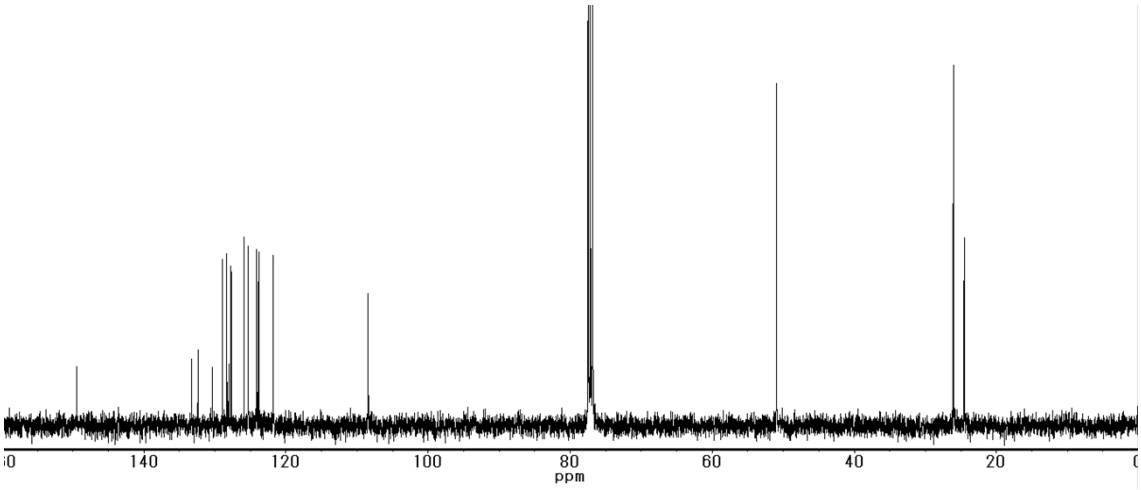

Fig. S10. ^{13}C NMR spectrum of **2-PA** (100 MHz, $CDCl_3$).

2,6-BPA

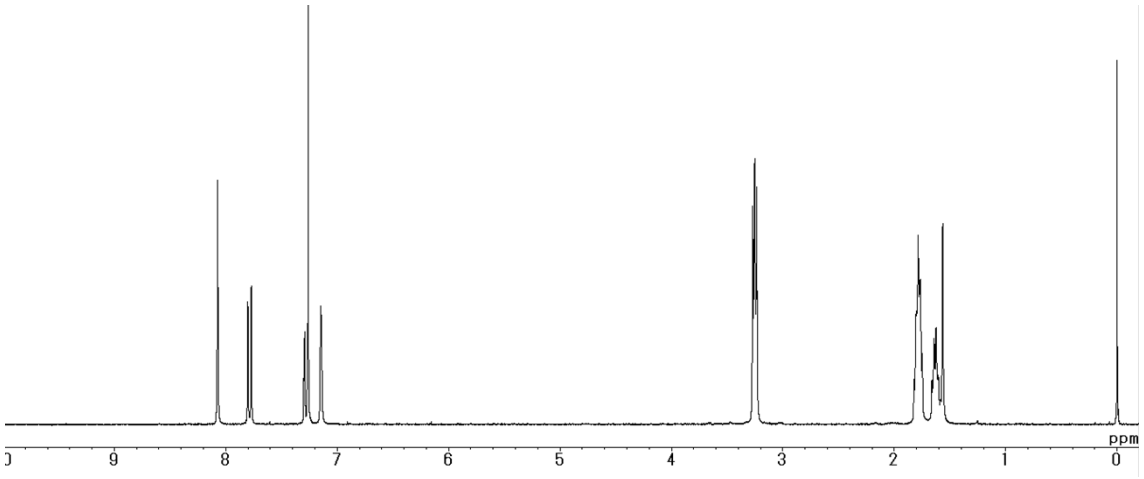

Fig. S11. ^{1}H NMR spectrum of **2,6-BPA** (300 MHz, $CDCl_3$).

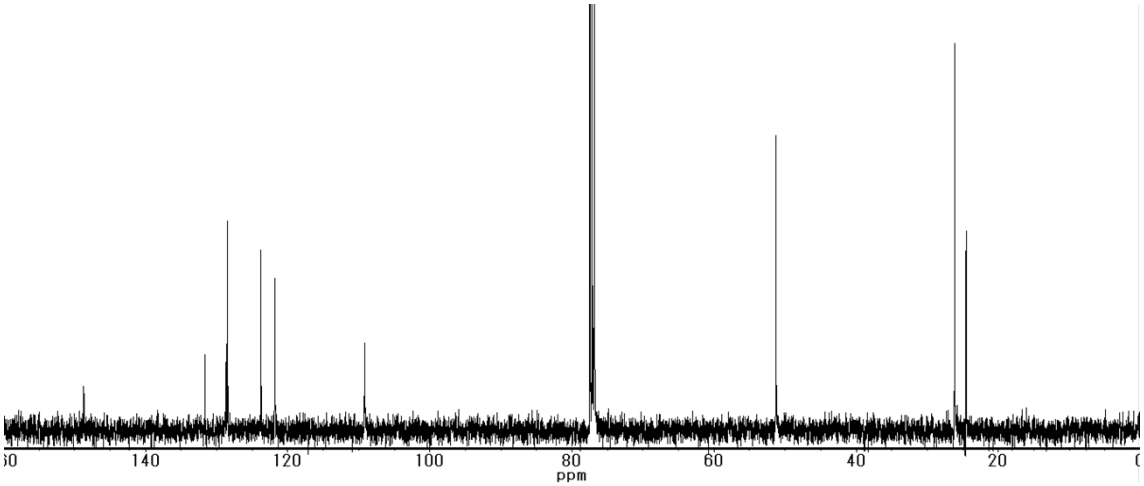

Fig. S12. ^{13}C NMR spectrum of **2,6-BPA** (100 MHz, $CDCl_3$).

9-PA

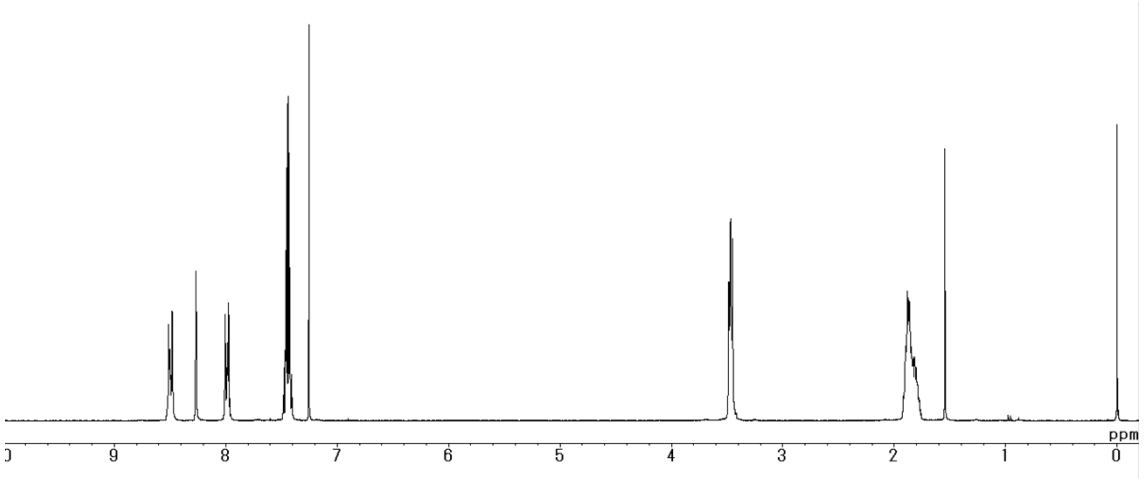

Fig. S13. ^{1}H NMR spectrum of **9-PA** (300 MHz, $CDCl_3$).

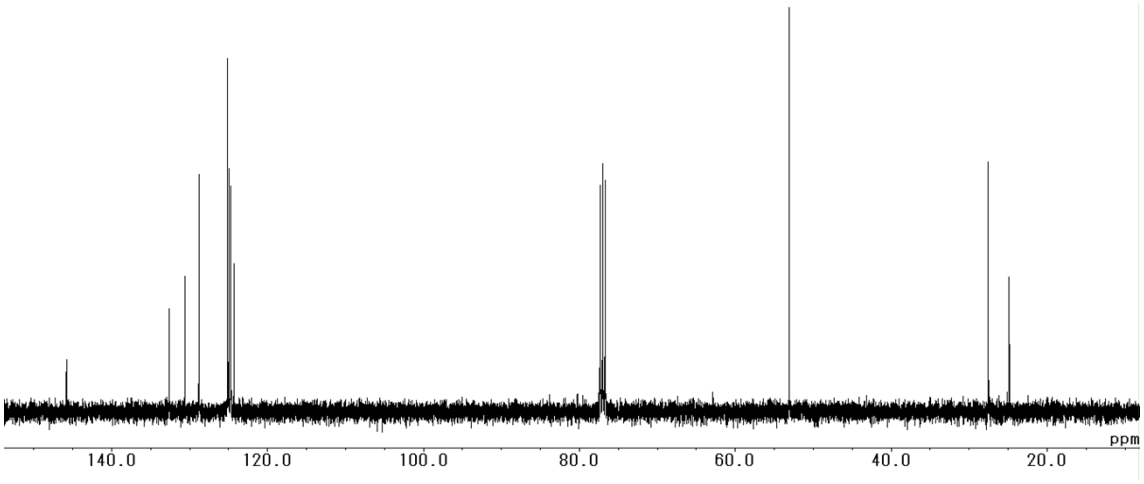

Fig. S14. ^{13}C NMR spectrum of **9-PA** (100 MHz, $CDCl_3$).

9,10-BPA

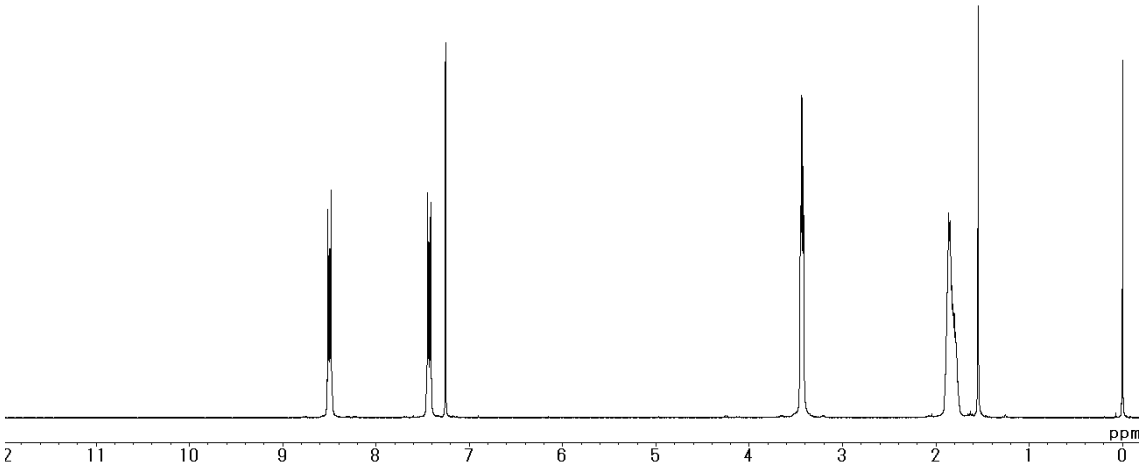

Fig. S15. ^{1}H NMR spectrum of **9,10-BPA** (300 MHz, $CDCl_3$).

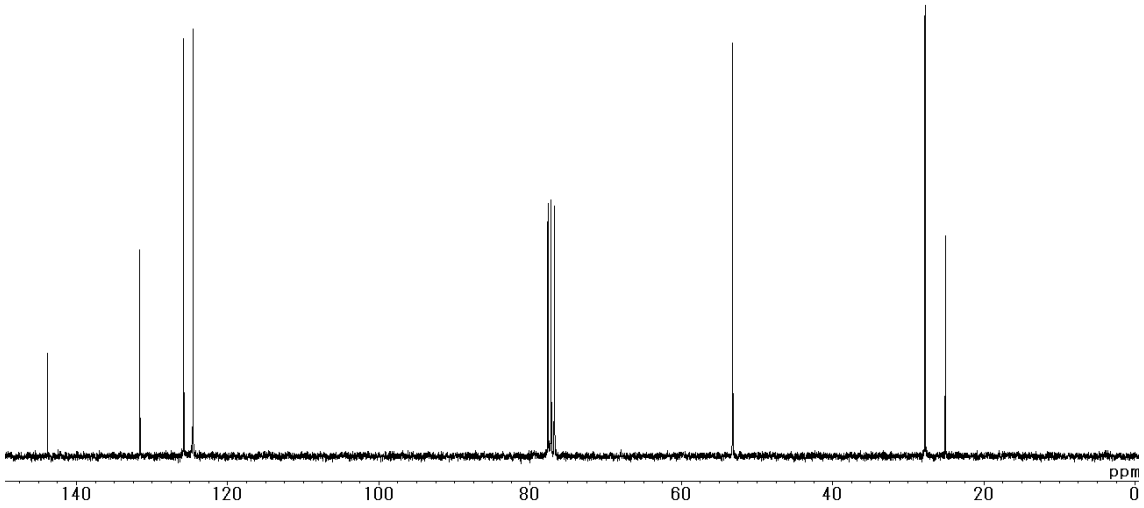

Fig. S16. ^{13}C NMR spectrum of **9,10-BPA** (75 MHz, $CDCl_3$).

S2. Thermogravimetric analysis (TGA)

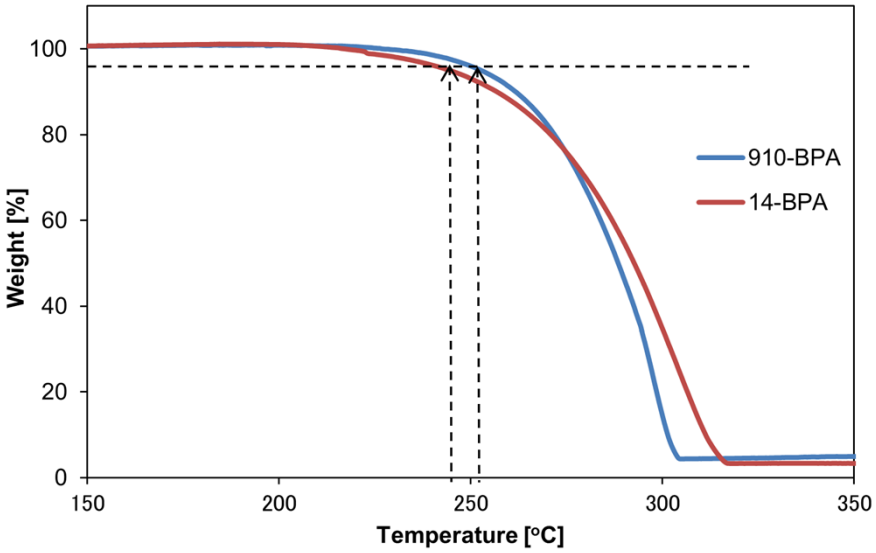

Fig. S17. TGA thermograms of AIE-active **1,4-BPA** and **9,10-BPA**.

S3. Dynamic light scattering (DLS) measurements

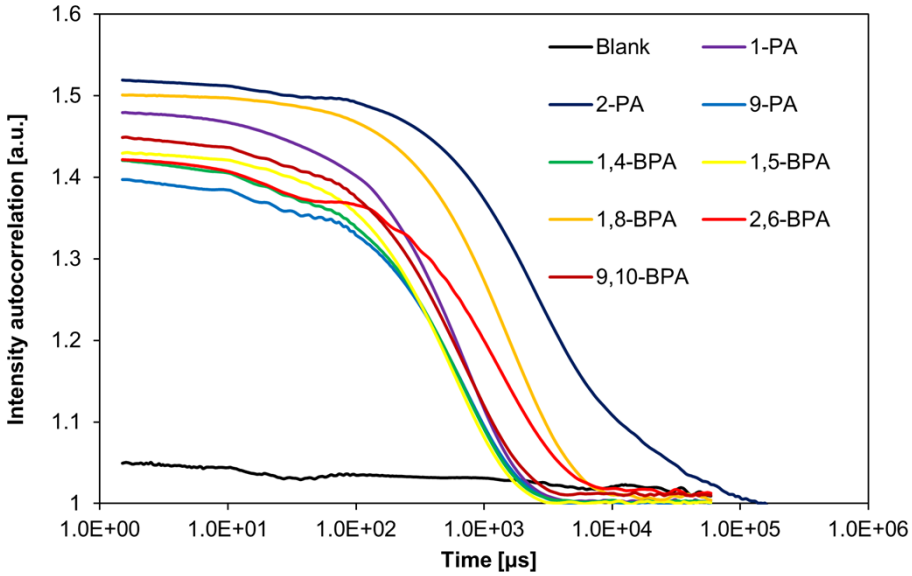

Fig. S18. Autocorrelation functions for the **PA** and **BPA** regioisomers plotted against the logarithm of the time decay ("Blank" data was obtained from the mixed THF: H_2O = 1:9 (v/v) solvent in the absence of analyte).

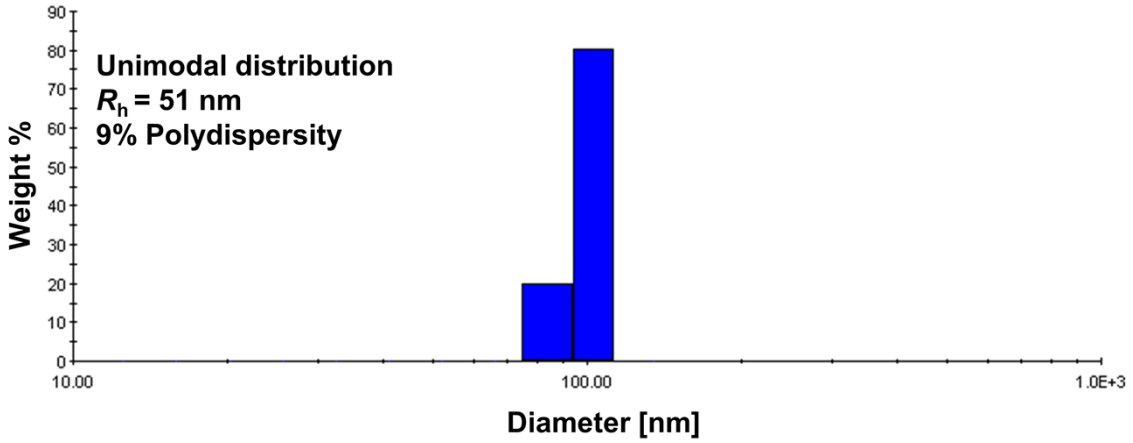

Fig. S19. Particle size distribution for **1-PA** calculated by regularisation analysis of its autocorrelation function.

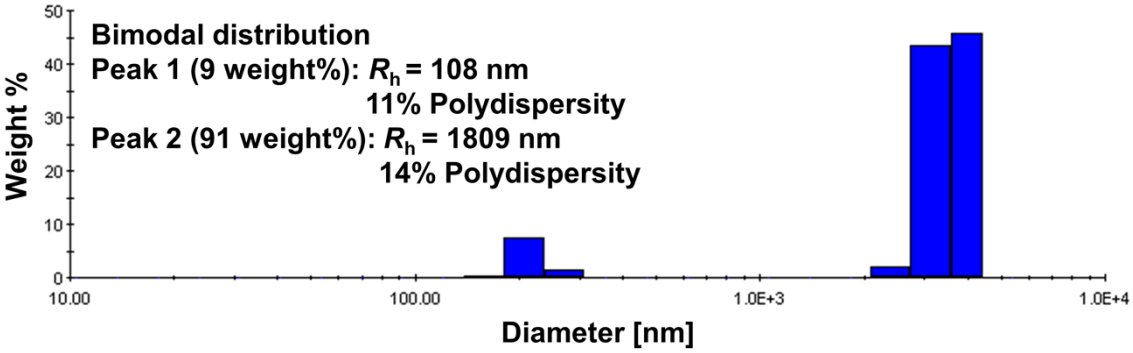

Fig. S20. Particle size distribution for **2-PA** calculated by regularisation analysis of its autocorrelation function.

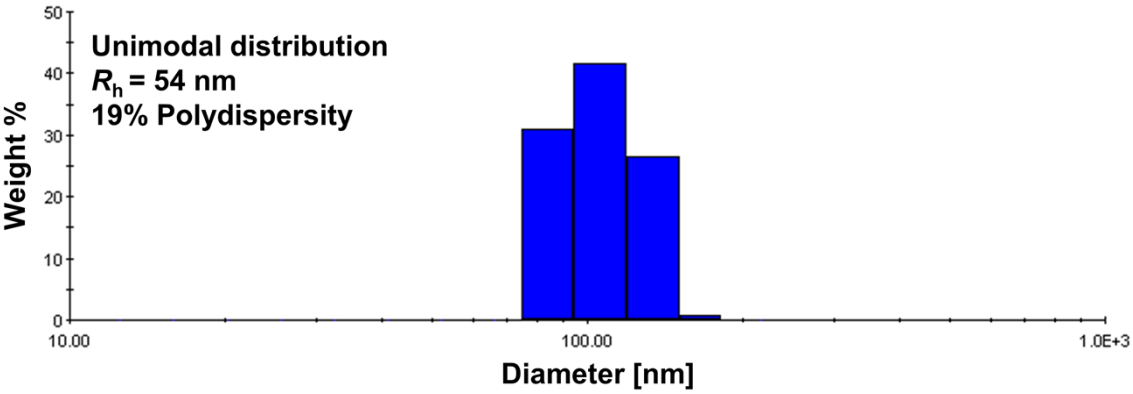

Fig. S21. Particle size distribution of **9-PA** calculated by regularisation analysis of its autocorrelation function.

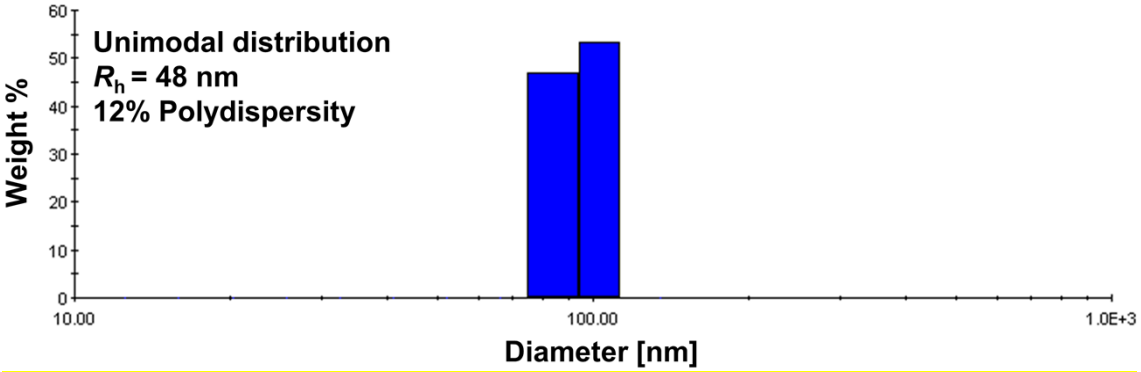

Fig. S22. Particle size distribution of **1,4-BPA** calculated by regularisation analysis of its autocorrelation function.

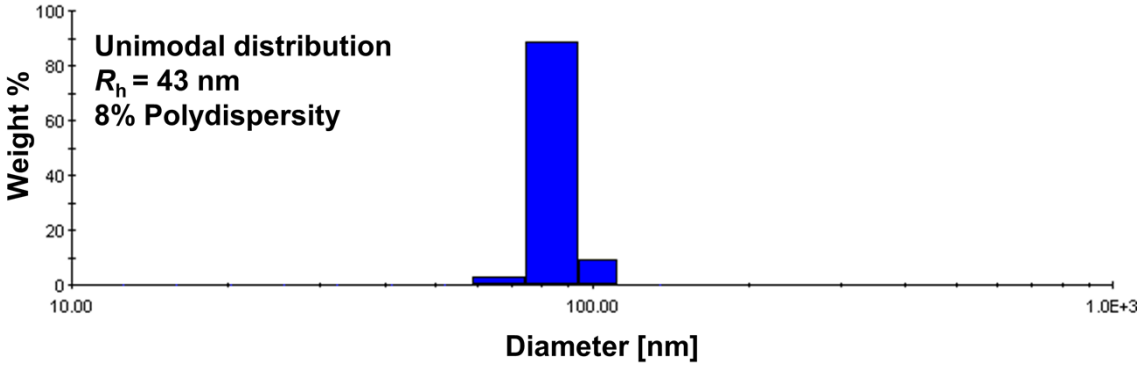

Fig. S23. Particle size distribution of **1,5-BPA** calculated by regularisation analysis of its autocorrelation function.

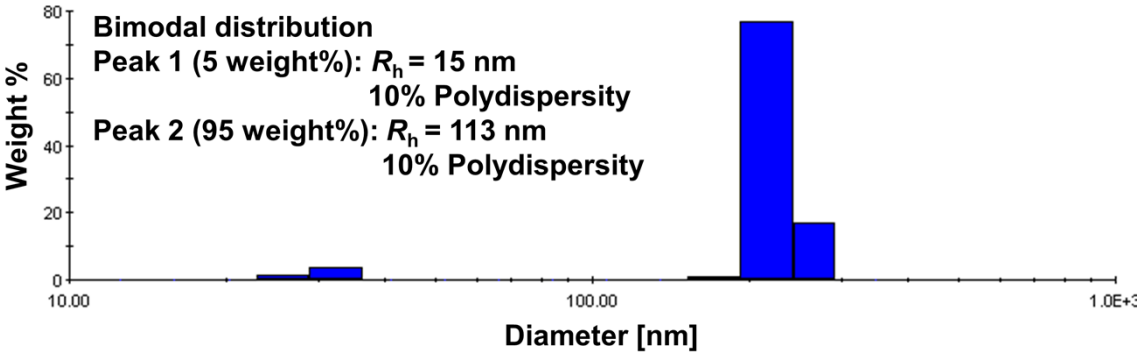

Fig. S24. Particle size distribution of **1,8-BPA** calculated by regularisation analysis of its autocorrelation function.

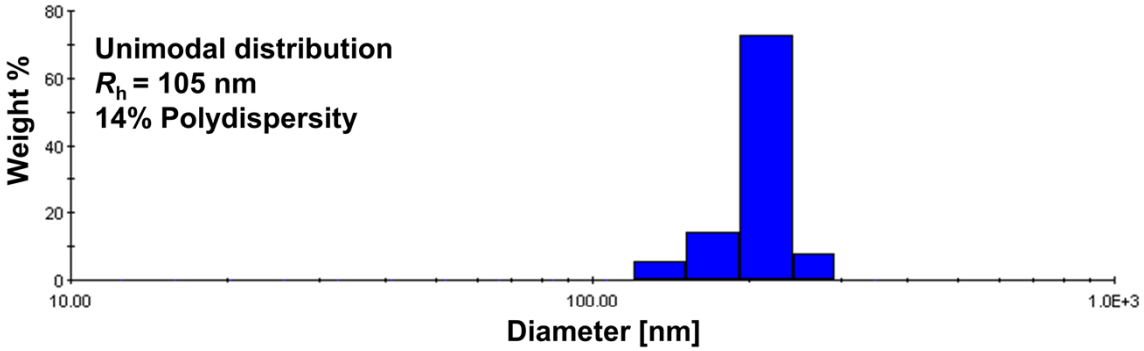

Fig. S25. Particle size distribution of **2,6-BPA** calculated by regularisation analysis of its autocorrelation function.

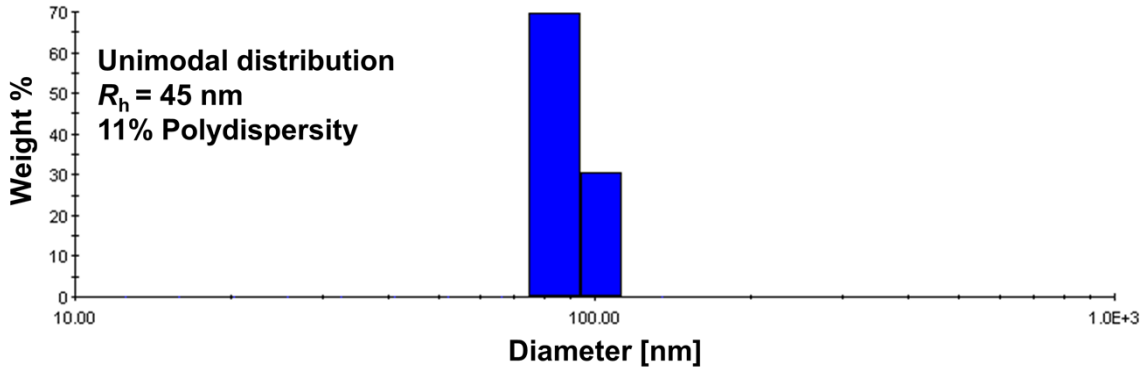

Fig. S26. Particle size distribution of **9,10-BPA** calculated by regularisation analysis of its autocorrelation function.

S4. Photophysical measurements

(1) Photophysical parameters

Table S1. Absorption maxima (λ_{abs}), fluorescence maxima (λ_{fl}), absolute fluorescence quantum yields (Φ_f), fluorescence lifetimes (τ_{fl}), radiative rate constants (k_r) and non-radiative rate constants (k_{nr}) for the regioisomers of **PA** and **BPA**.

Entry	Solvent	ε [M^{-1} cm^{-1}]	λ_{abs} [nm]	λ_{fl}[a] [nm]	Φ_f[b]	τ_{fl}[d] [ns]	k_f [10^6 s^{-1}]	k_{nr} [10^6 s^{-1}]
1-PA	Toluene	5200	387	504	0.862	15.2	57	9.1
	THF	5100	385	521	0.905	17.1	53	5.6
	DMF	5000	387	550	0.847	23.8	36	6.4
	THF-H_2O[c]	-	402	519	0.487	2.6 (0.10) 14.1 (0.90)	37[e]	40[e]
1,4-BPA	Toluene	5600	403	587	0.447	13.1	34	42
	THF	5700	401	598	0.251	9.9	25	76
	DMF	5400	404	631	0.080	-	-	-
	THF-H_2O[c]	-	414	596	0.446	18.4	24[e]	30[e]
1,5-BPA	Toluene	7300	390	490	0.589	8.4	70	49
	THF	7400	389	504	0.767	11.5	67	20
	DMF	7100	392	533	0.867	18.6	47	7.2
	THF-H_2O[c]	-	415	504	0.120	1.0 (0.50) 3.9 (0.50)	49[e]	360[e]
1,8-BPA	Toluene	6400	387	498	0.592	10.6	56	39
	THF	6400	385	514	0.705	14.6	48	20
	DMF	6300	388	540	0.795	21.1	38	9.7
	THF-H_2O[c]	-	397	514	0.152	2.0 (0.33) 6.4 (0.67)	31[e]	170[e]
2-PA	Toluene	3600[f]	400, 339	489[g]	0.936	16.6	56	3.9
	THF	3600[f]	399, 338	504[g]	0.909	17.1	53	5.3
	DMF	3500[f]	402, 339	525[g]	0.923	22.9	40	3.4
	THF-H_2O[c]		428, 365	488[g]	0.339	3.6 (0.22) 8.8 (0.78)	45[e]	87[e]
2,6-BPA	Toluene	5100[f]	423, 335	513[g]	0.925	15.5	60	4.9
	THF	5200[f]	423, 335	515[g]	0.883	16.2	54	7.2
	DMF	5100[f]	428, 336	528[g]	0.921	20.1	46	3.9
	THF-H_2O[c]		440, 341	504[g]	0.147	1.4 (0.50) 5.5 (0.50)	43[e]	250[e]
9-PA	Toluene	6000	388	472	0.011	-	-	-
	THF	6100	387	478	0.008	-	-	-
	DMF	5700	388	495	0.013	-	-	-
	THF-H_2O[c]	-	394	490	0.047	-	-	-
9,10-BPA	Toluene	5800	400	525	0.024	-	-	-
	THF	6100	399	528	0.021	-	-	-
	DMF	5600	400	537	0.019	-	-	-
	THF-H_2O[c]	-	407	514	0.789	4.3 (0.05) 12.1 (0.95)	67[e]	18[e]

[a] Excitation wavelengths correspond to the absorption maxima of the band with the longest wavelength.

[b] The excitation wavelength was fixed at 343 nm, which is the wavelength of the light source of the lifetime spectrometer. All of these quantum yields are almost identical to those collected when excitation wavelengths correspond to the absorption maxima at the band with the longest wavelength.

[c] THF:H_2O = 1:9 (v/v); the formation of aggregation was confirmed by broadening of the corresponding UV-Vis spectra (Fig. S27-S34).
[d] The values in brackets indicate relative contributions of each lifetime component.
[e] Average lifetime amplitudes were used for the calculations.[1]
[f] Extinction coefficients at the band with the longest wavelength.
[g] Fluorescence spectra did not show any significant change as a function of the excitation wavelength (Fig. S39-S42).

Table S2. Maxima of diffuse-reflectance spectra (λ_{df}), fluorescence maxima (λ_{fl}), absolute fluorescence quantum yields (Φ_f), and Stokes shifts ($\Delta\tilde{\upsilon}_{St}$) of the **PA** and **BPA** regioisomers.

Entry	State	λ_{df} [nm]	λ_{fl}[a] [nm]	Φ_f[b]	$\Delta\tilde{\upsilon}_{St}$ [cm^{-1}]
1-PA	1mM in NaBr[c]	394	495	-	5300
	Neat powder	-	500	0.522	-
1,4-BPA	1mM in NaBr[c]	414	594	-	7400
	Neat powder	-	591	0.492	-
1,5-BPA	1mM in NaBr[c]	397	495	-	5200
	Neat powder	-	518	0.344	-
1,8-BPA	1mM in NaBr[c]	395	500	-	5800
	Neat powder	-	531	0.123	-
2-PA	1mM in NaBr[c]	431	497	-	3200
	Neat powder	-	523	0.267	-
2,6-BPA	1mM in NaBr[c]	436	508	-	3600
	Neat powder	-	532	0.174	-
9-PA	1mM in NaBr[c]	394	519	-	6400
	Neat powder	-	519	0.709	-
9,10-BPA	1mM in NaBr[c]	404	519	-	5500
	Neat powder	-	519	0.856	-

[a] The excitation wavelength corresponds to the maxima of diffused-reflectance spectra observed from the dispersed state in NaBr.
[b] Excitation wavelength: 350 nm. For those with different excitation wavelengths, see Fig. S35-S42.
[c] Samples adsorbed on NaBr powder at a concentration of $1.0 \cdot 10^{-3}$ M.

(2) Absorption spectra

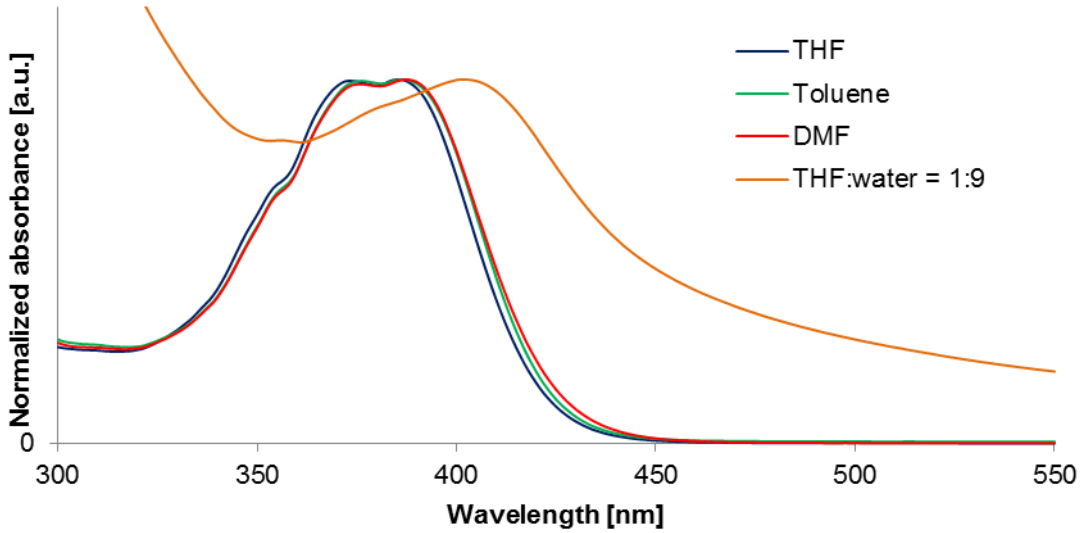

Fig. S27. UV-Vis absorption spectra of **1-PA**.

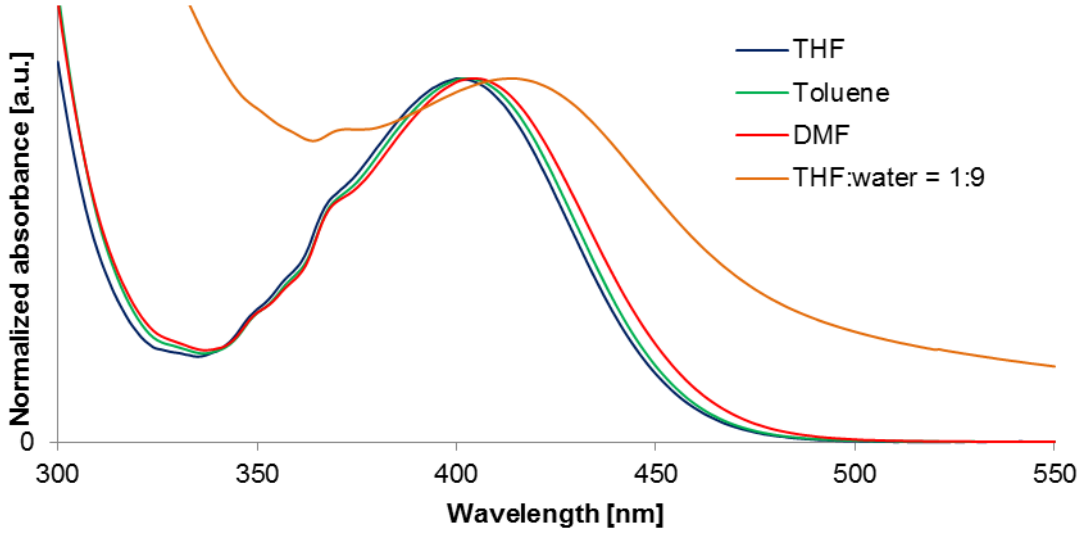

Fig. S28. UV-Vis absorption spectra of **1,4-BPA**.

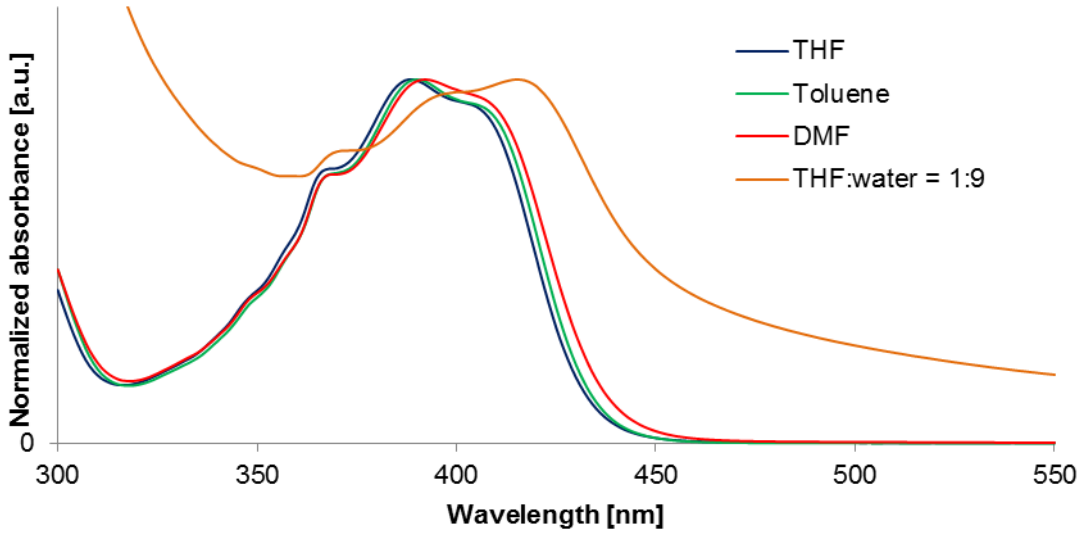

Fig. S29. UV-Vis absorption spectra of **1,5-BPA**.

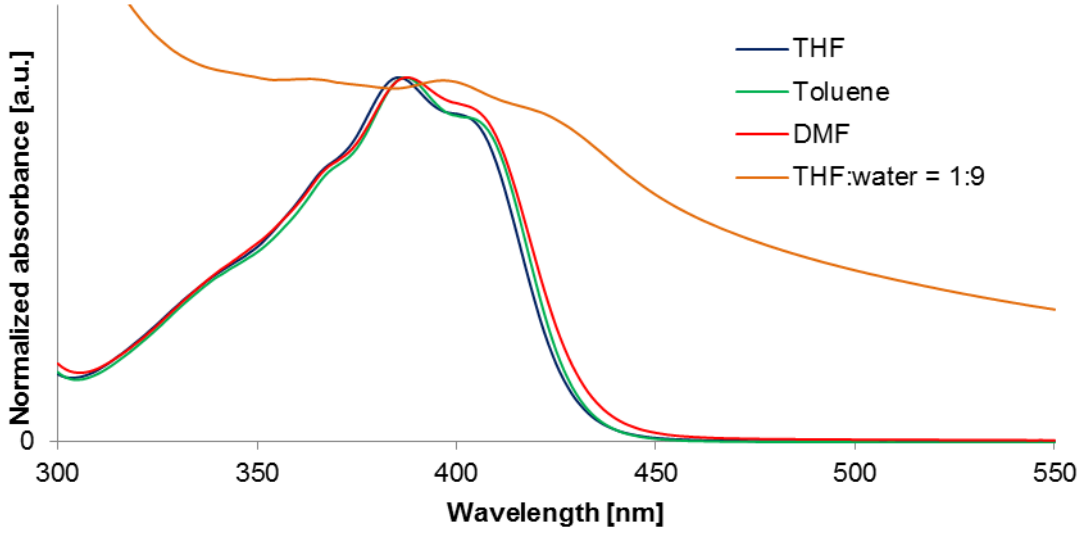

Fig. S30. UV-Vis absorption spectra of **1,8-BPA**.

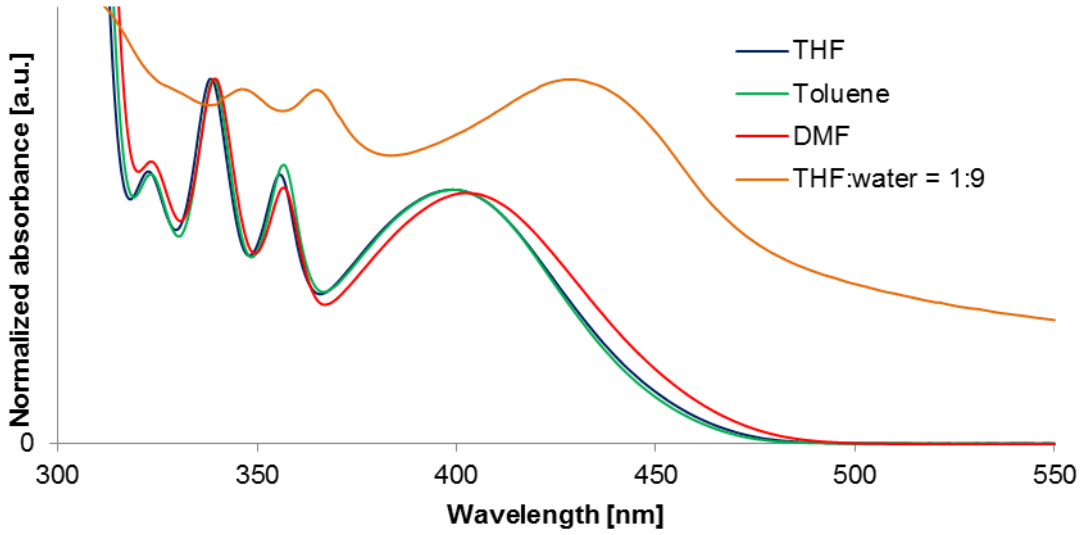

Fig. S31. UV-Vis absorption spectra of **2-PA**.

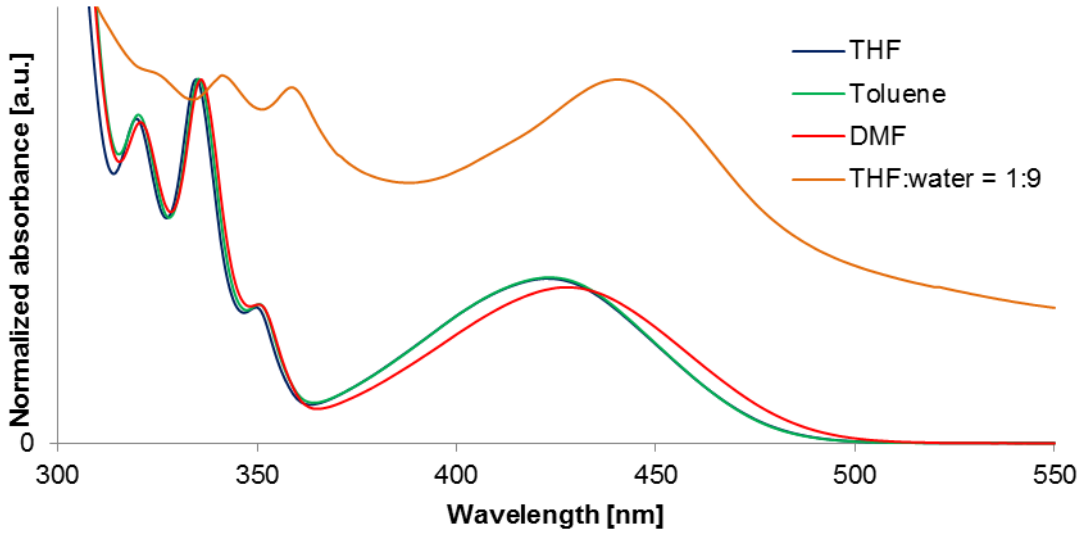

Fig. S32. UV-Vis absorption spectra of **2,6-BPA**.

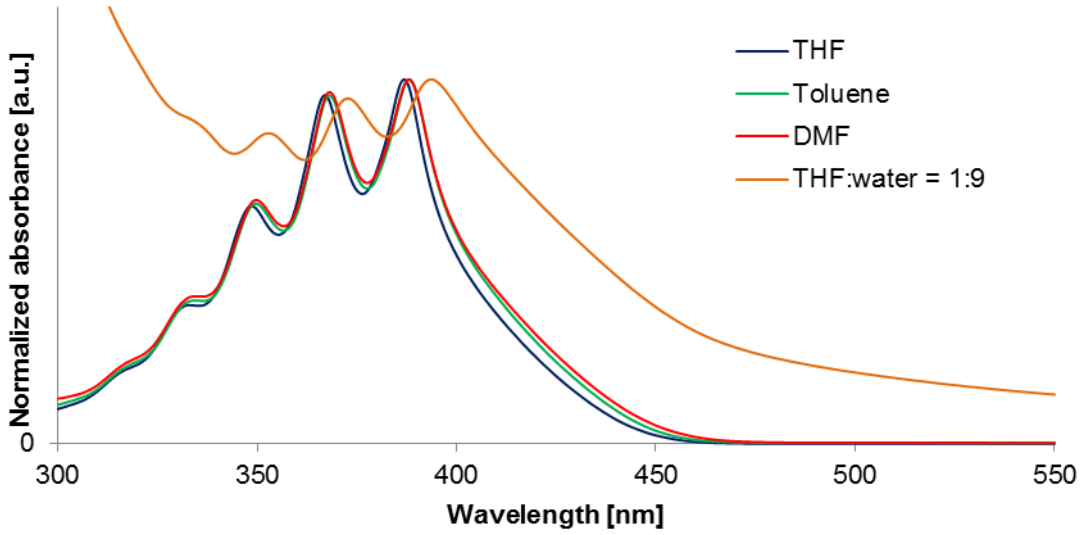

Fig. S33. UV-Vis absorption spectra of **9-PA**.

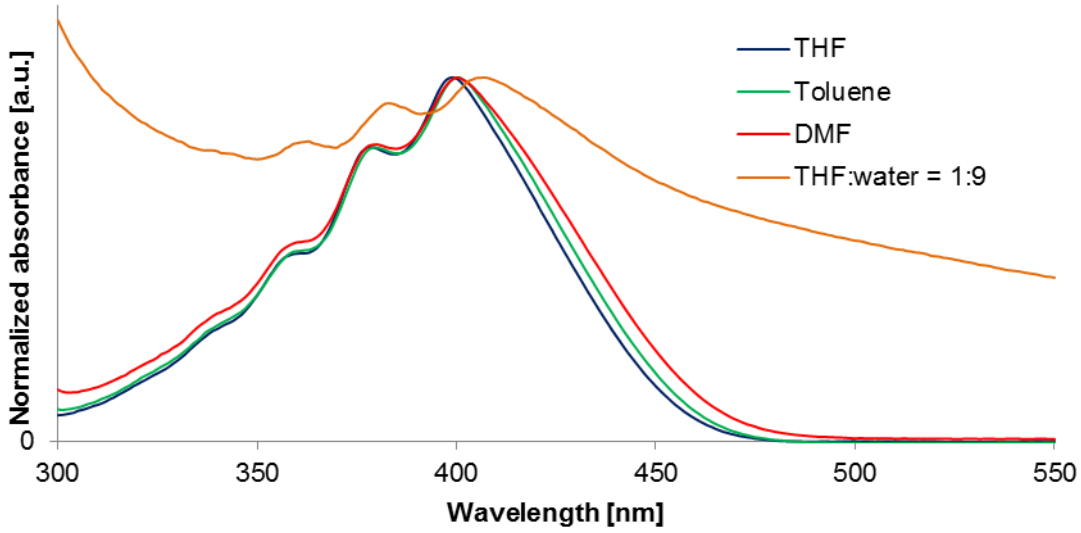

Fig. S34. UV-Vis absorption spectra of **9,10-BPA**.

(3) Fluorescence spectra

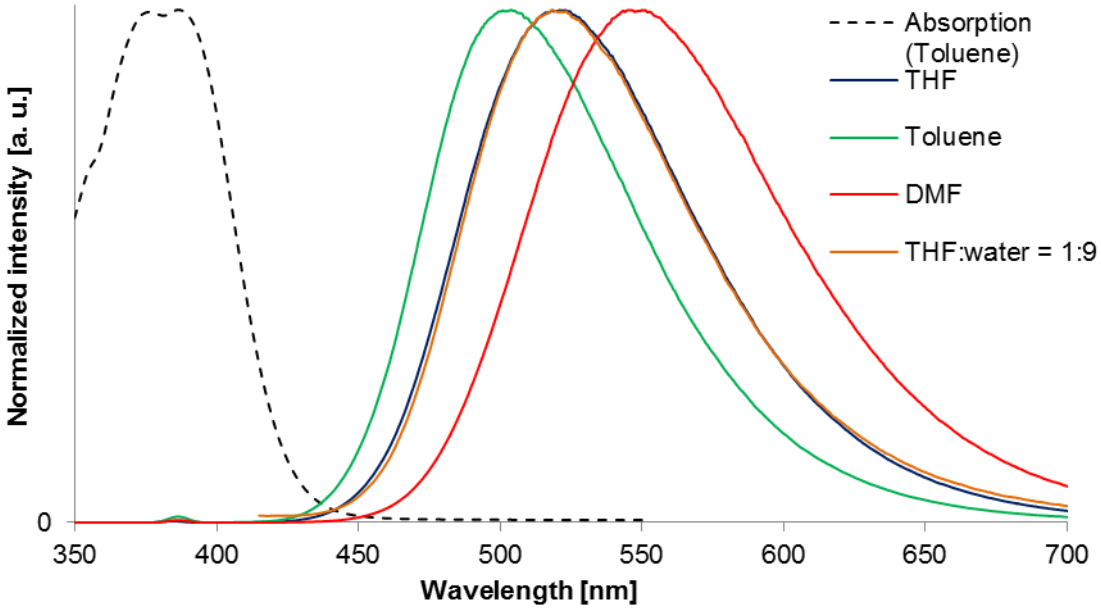

Fig. S35. Fluorescence spectra of **1-PA**.

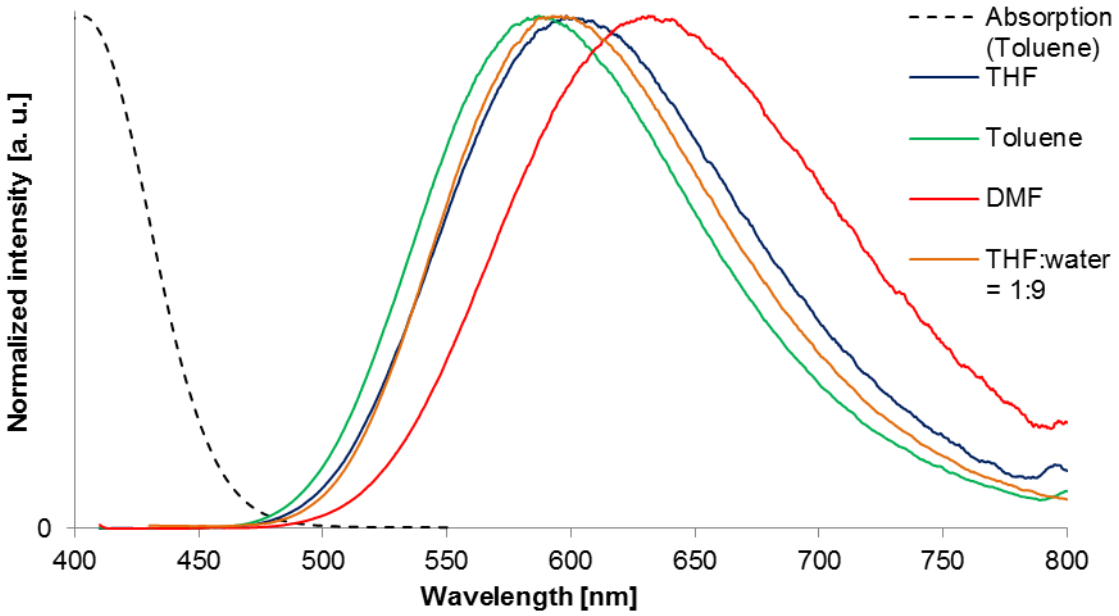

Fig. S36. Fluorescence spectra of **1,4-BPA**.

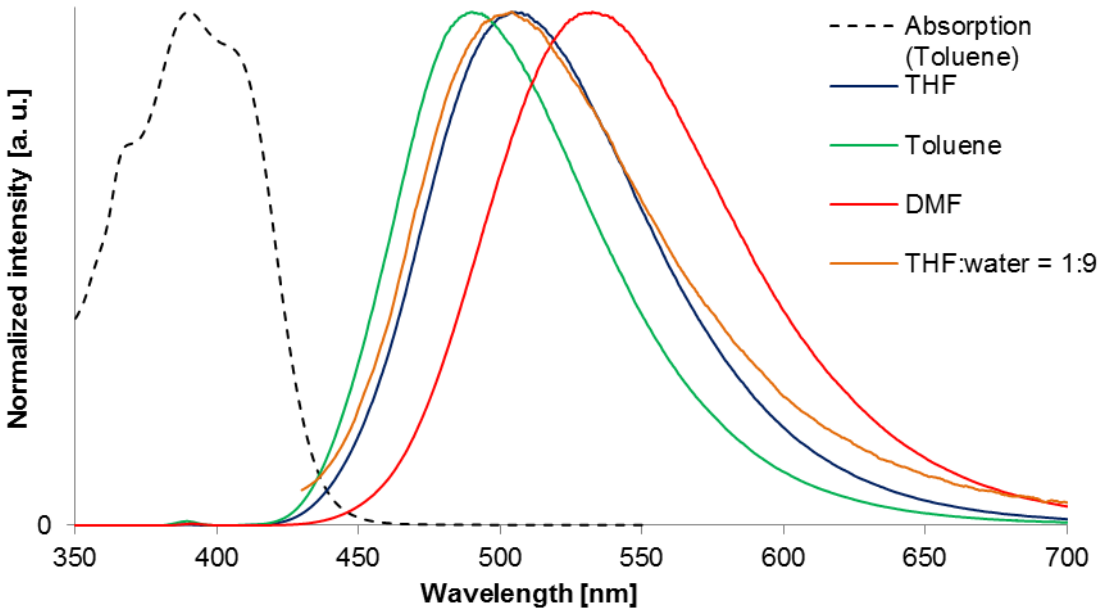

Fig. S37. Fluorescence spectra of **1,5-BPA**.

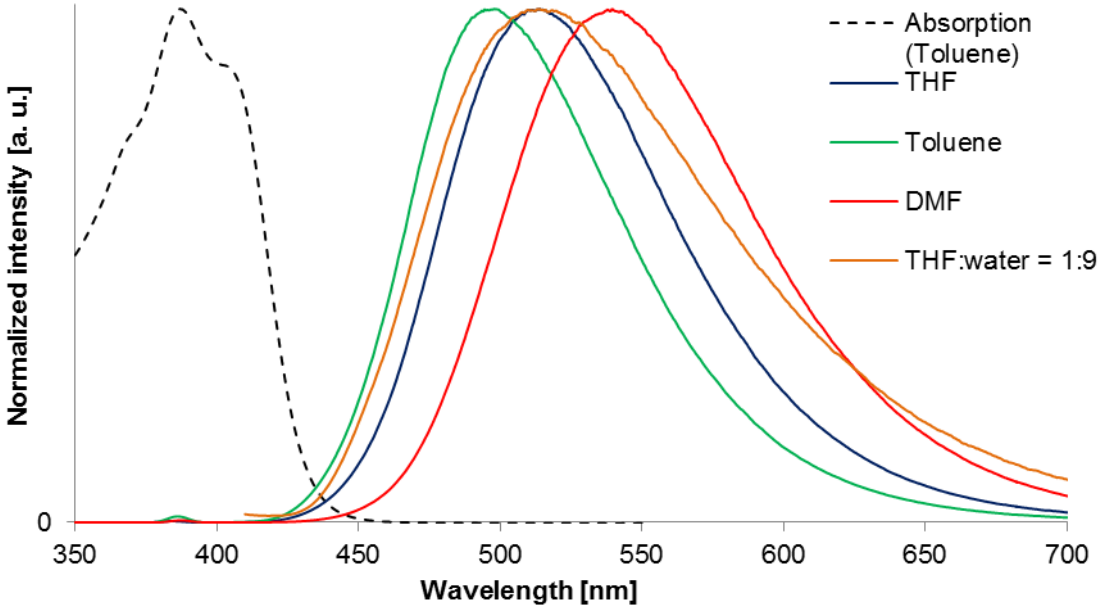

Fig. S38. Fluorescence spectra of **1,8-BPA**.

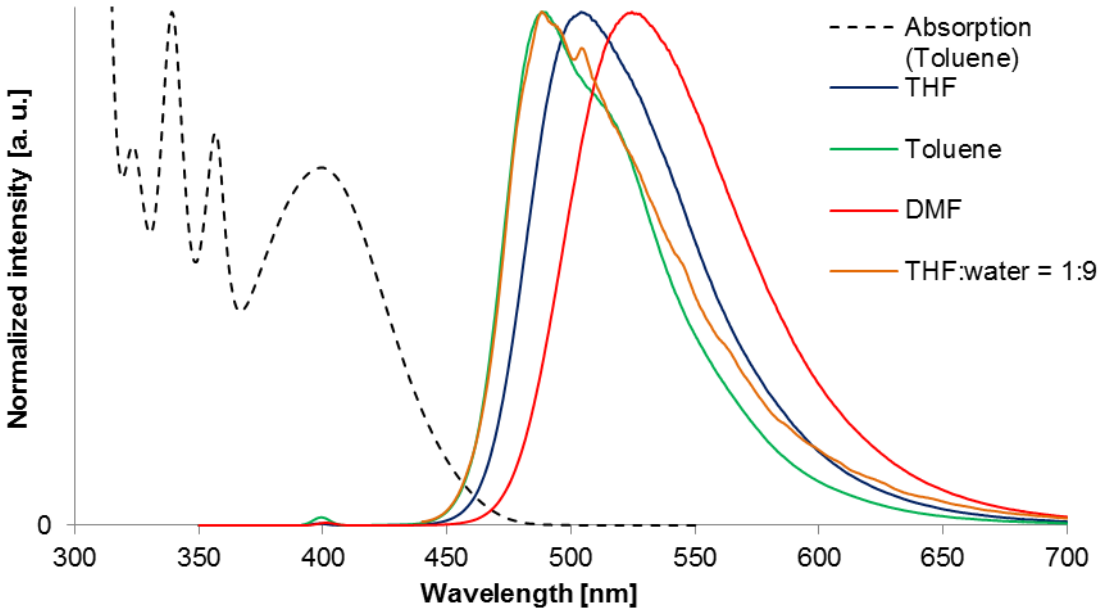

Fig. S39. Fluorescence spectra of **2-PA** (excitation wavelength of these spectra correspond to maxima of longer-wavelength bands around 400 nm).

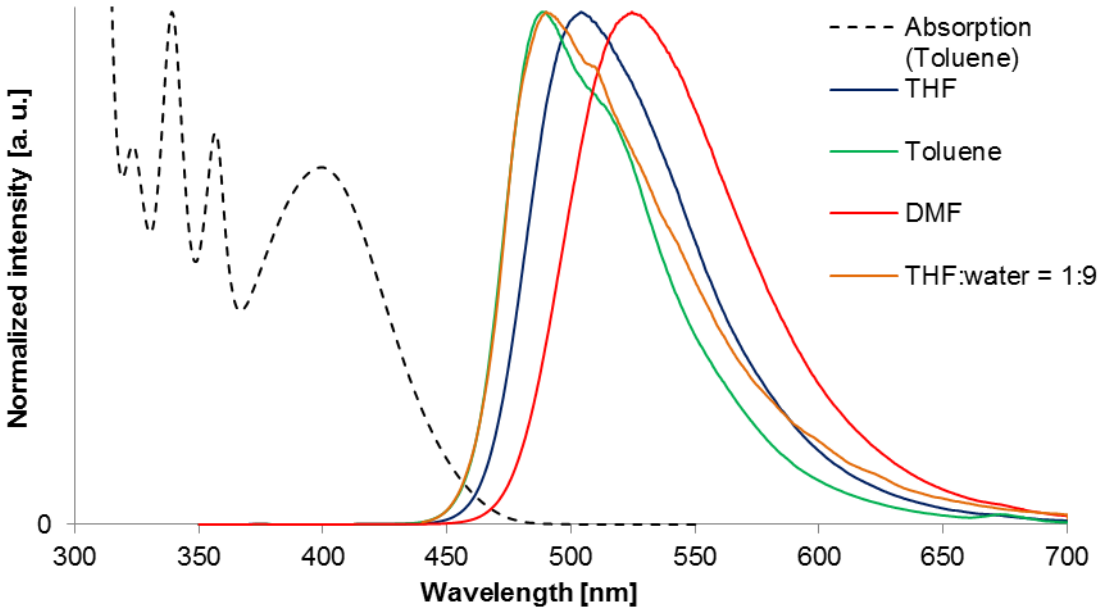

Fig. S40. Fluorescence spectra of **2-PA** (excitation wavelengths of these spectra correspond to maxima of shorter-wavelength bands around 340 nm).

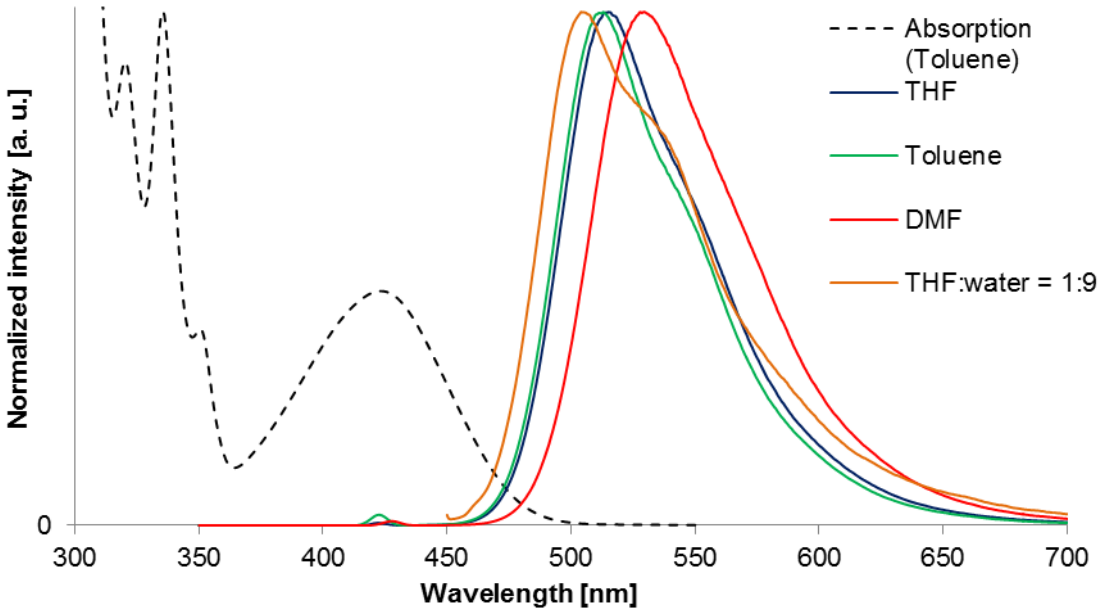

Fig. S41. Fluorescence spectra of **2,6-BPA** (excitation wavelengths of these spectra correspond to maxima of longer-wavelength bands around 420 nm).

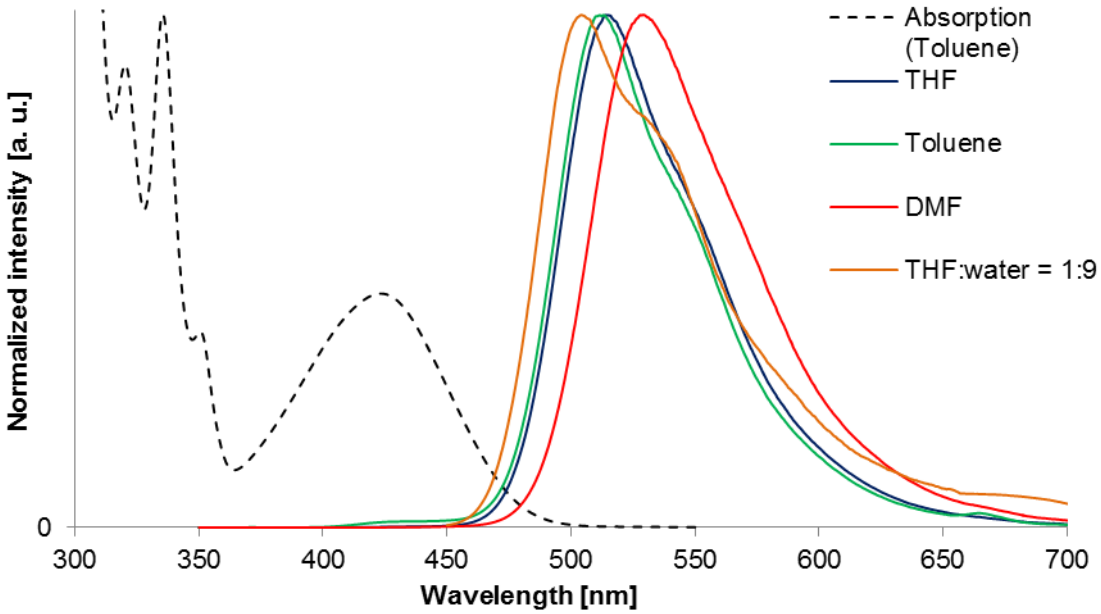

Fig. S42. Fluorescence spectra of **2,6-BPA** (excitation wavelengths of these spectra correspond to maxima of longer-wavelength bands around 340 nm).

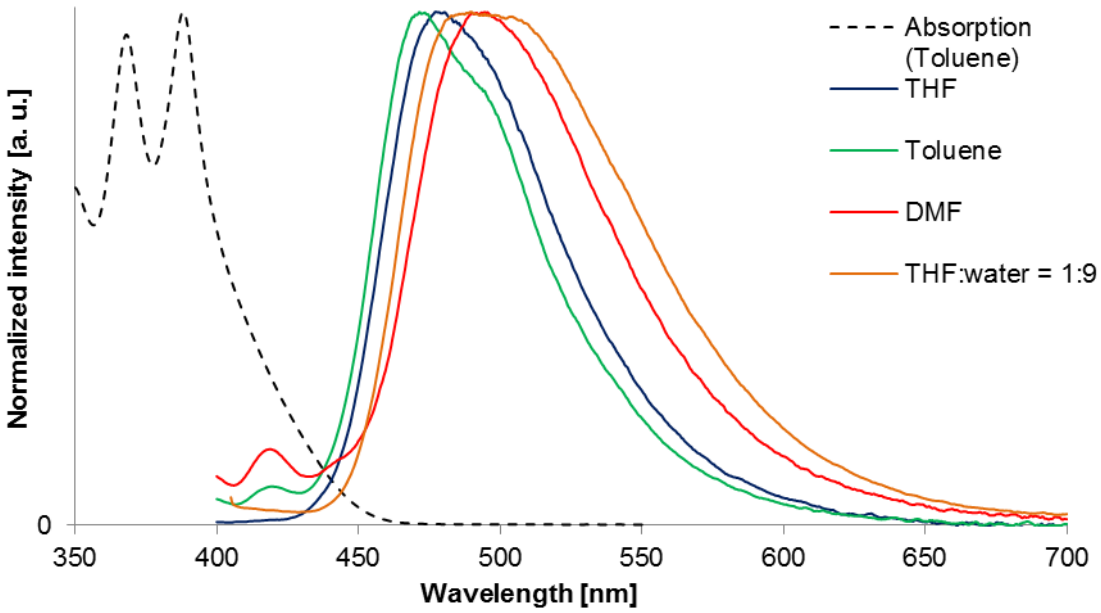

Fig. S43. Fluorescence spectra of **9-PA**.

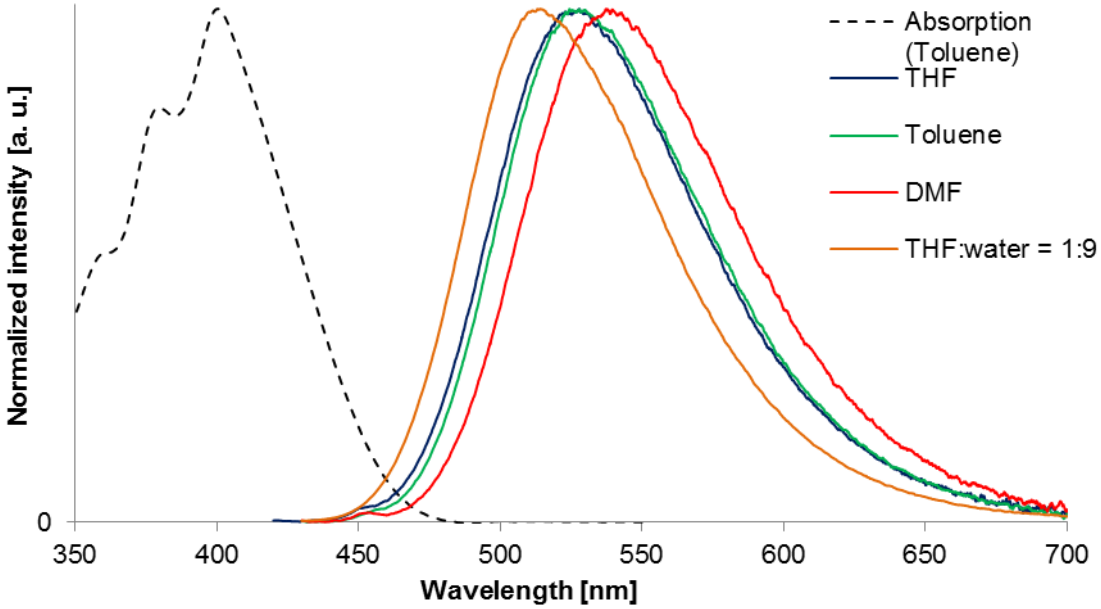

Fig. S44. Fluorescence spectra of **9,10-BPA**.

(4) Diffuse-reflectance spectra of polycrystalline solids

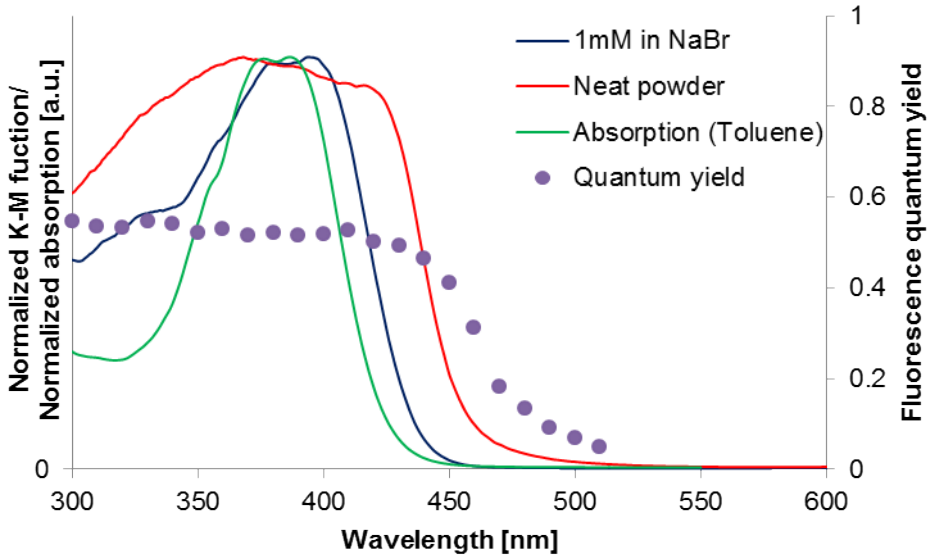

Fig. S45. Diffuse-reflectance spectra and excitation-wavelength dependency of the fluorescence quantum yield, Φ_f, (neat powder) obtained from **1-PA**.

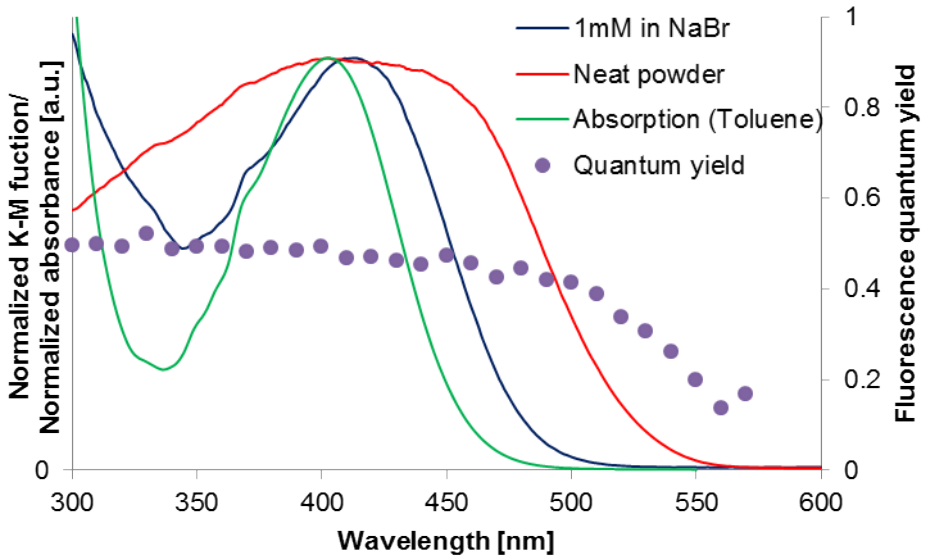

Fig. S46. Diffuse-reflectance spectra and excitation-wavelength dependency of the fluorescence quantum yield, Φ_f, (neat powder) obtained from **1,4-BPA**.

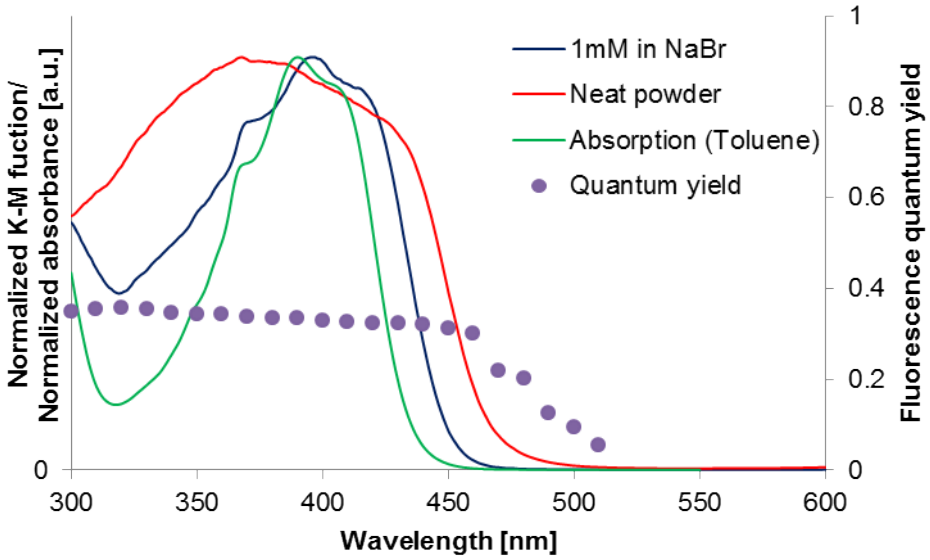

Fig. S47. Diffuse-reflectance spectra and excitation-wavelength dependency of the fluorescence quantum yield, *Φ*f, (neat powder) obtained from **1,5-BPA**.

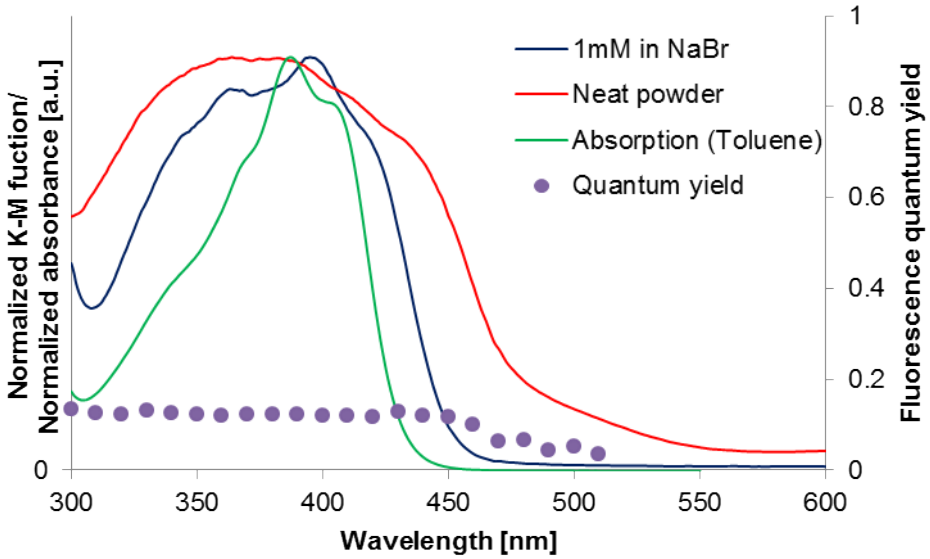

Fig. S48. Diffuse-reflectance spectra and excitation-wavelength dependency of the fluorescence quantum yield, *Φ*f, (neat powder) obtained from **1,8-BPA**.

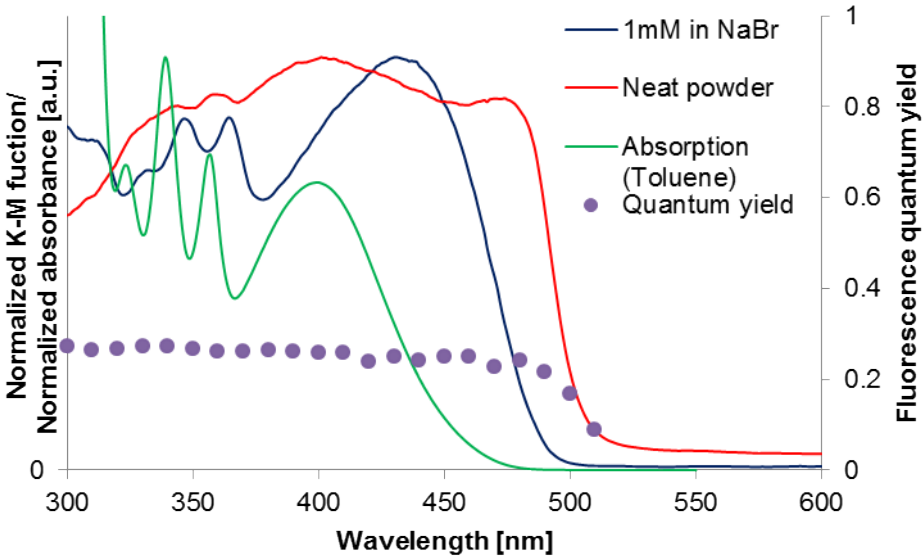

Fig. S49. Diffuse-reflectance spectra and excitation-wavelength dependency of the fluorescence quantum yield, *Φ*f, (neat powder) obtained from **2-PA**.

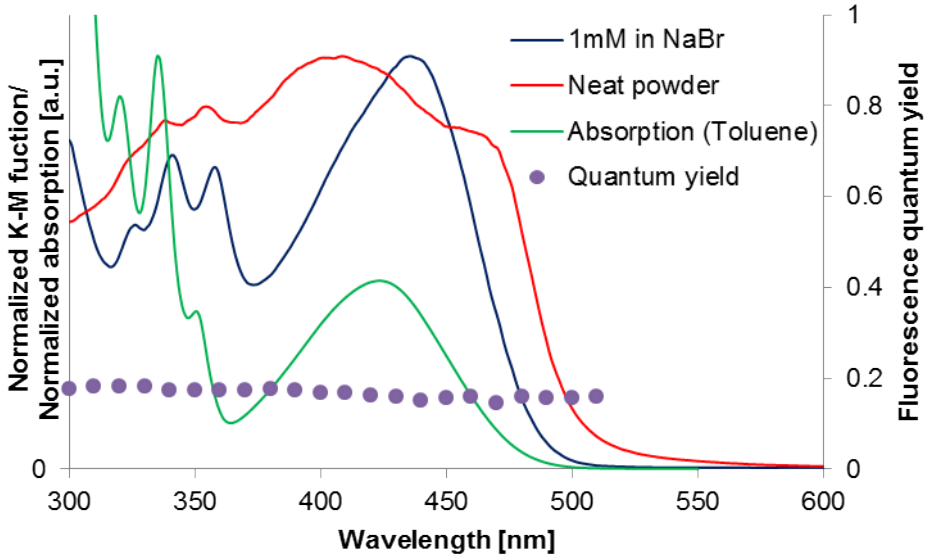

Fig. S50. Diffuse-reflectance spectra and excitation-wavelength dependency of the fluorescence quantum yield, *Φ*f, (neat powder) obtained from **2,6-BPA**.

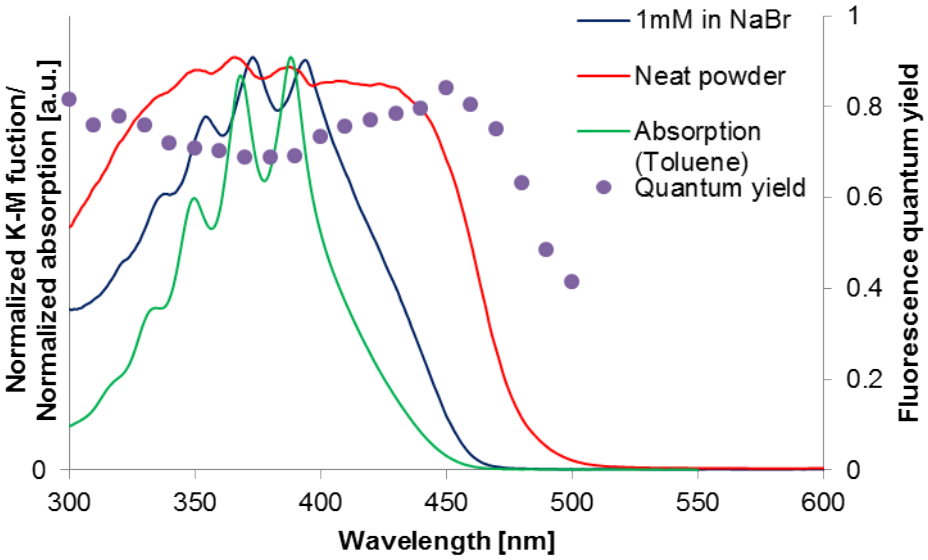

Fig. S51. Diffuse-reflectance spectra and excitation-wavelength dependency of the fluorescence quantum yield, Φf, (neat powder) obtained from **9-PA**.

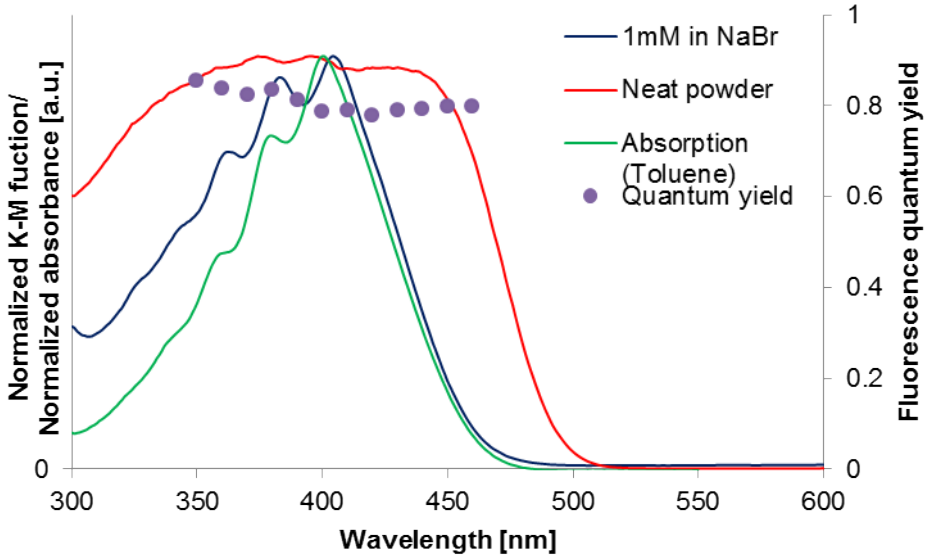

Fig. S52. Diffuse-reflectance spectra and excitation-wavelength dependency of the fluorescence quantum yield, Φf, (neat powder) obtained from **9,10-BPA**.

(5) Fluorescence spectra in the solid state

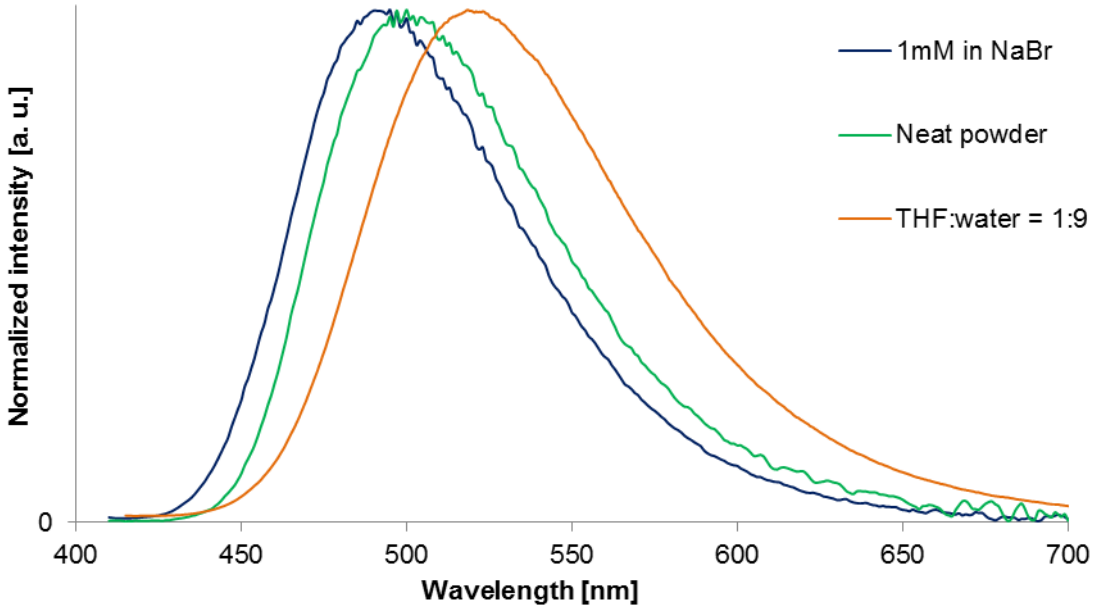

Fig. S53. Fluorescence spectra of **1-PA** in the solid state (the excitation wavelength corresponds to the maxima of diffused-reflectance spectra observed from the dispersed state in NaBr).

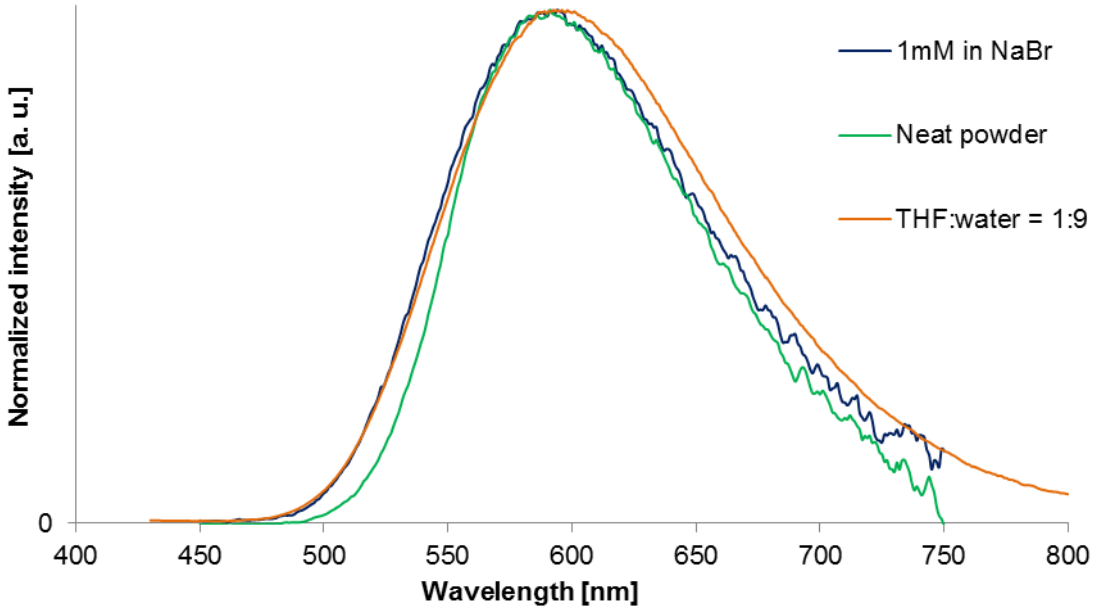

Fig. S54. Fluorescence spectra of **1,4-BPA** in the solid state (the excitation wavelength corresponds to the maxima of diffused-reflectance spectra observed from the dispersed state in NaBr).

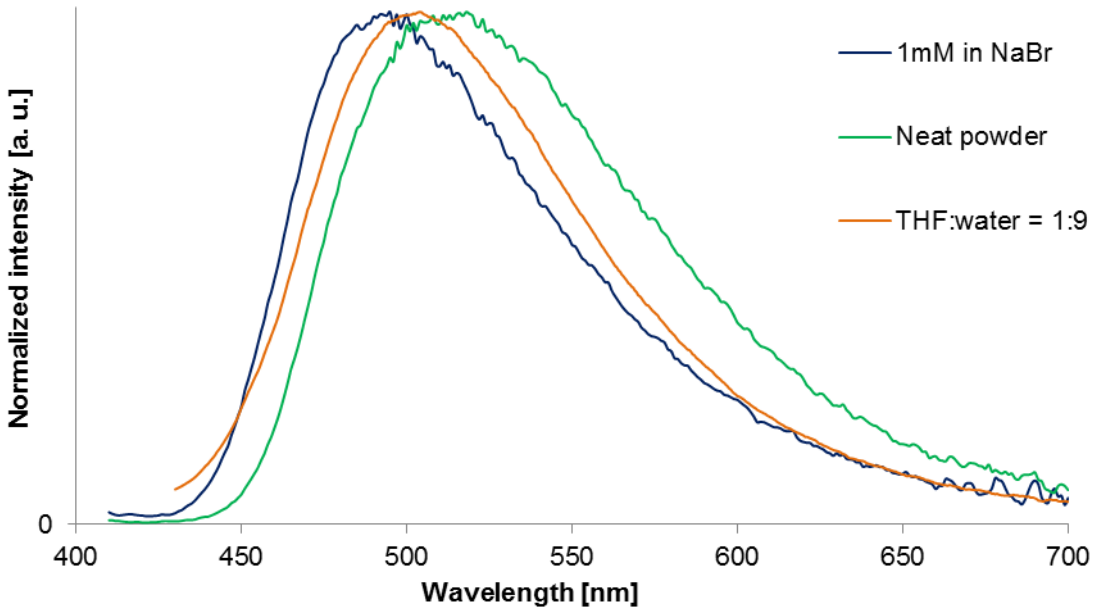

Fig. S55. Fluorescence spectra of **1,5-BPA** in the solid state (the excitation wavelength corresponds to the maxima of diffused-reflectance spectra observed from the dispersed state in NaBr).

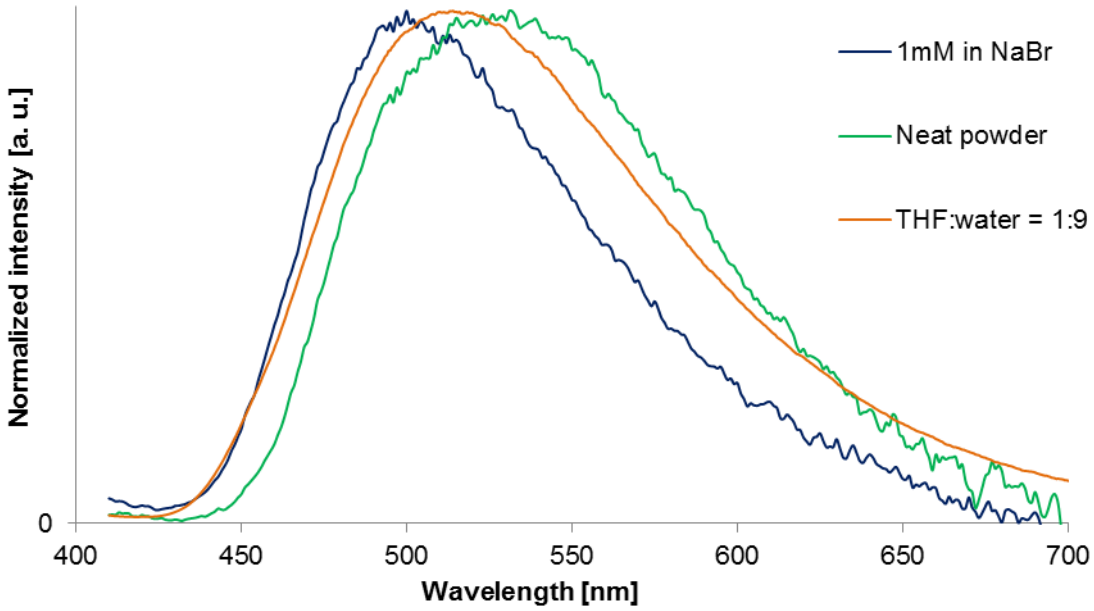

Fig. S56. Fluorescence spectra of **1,8-BPA** in the solid state (the excitation wavelength corresponds to the maxima of diffused-reflectance spectra observed from the dispersed state in NaBr).

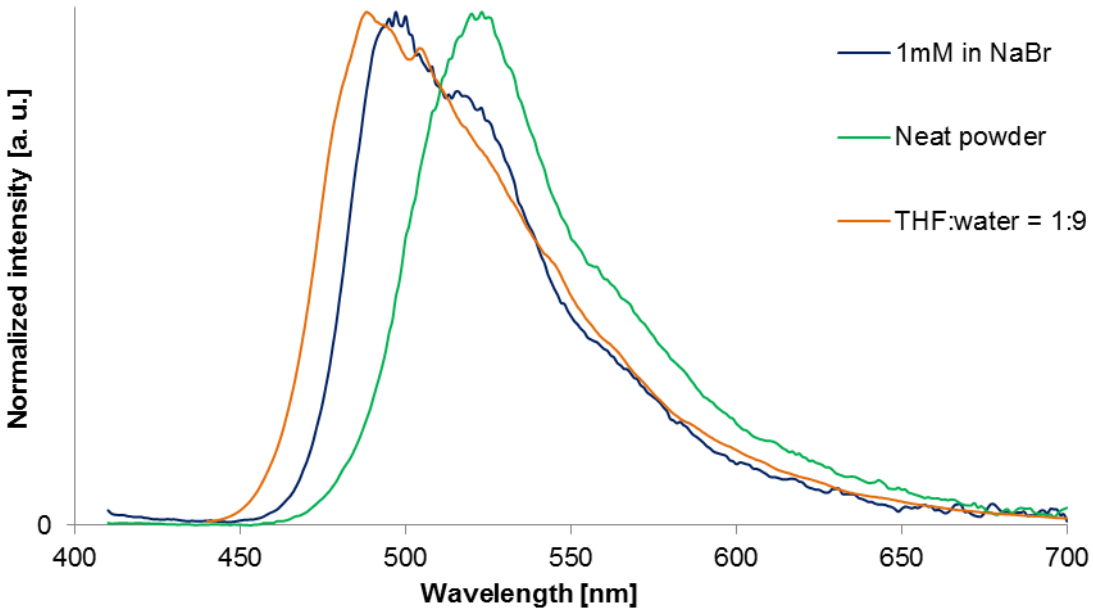

Fig. S57. Fluorescence spectra of **2-PA** in the solid state (the excitation wavelength corresponds to the maxima of diffused-reflectance spectra observed from the dispersed state in NaBr).

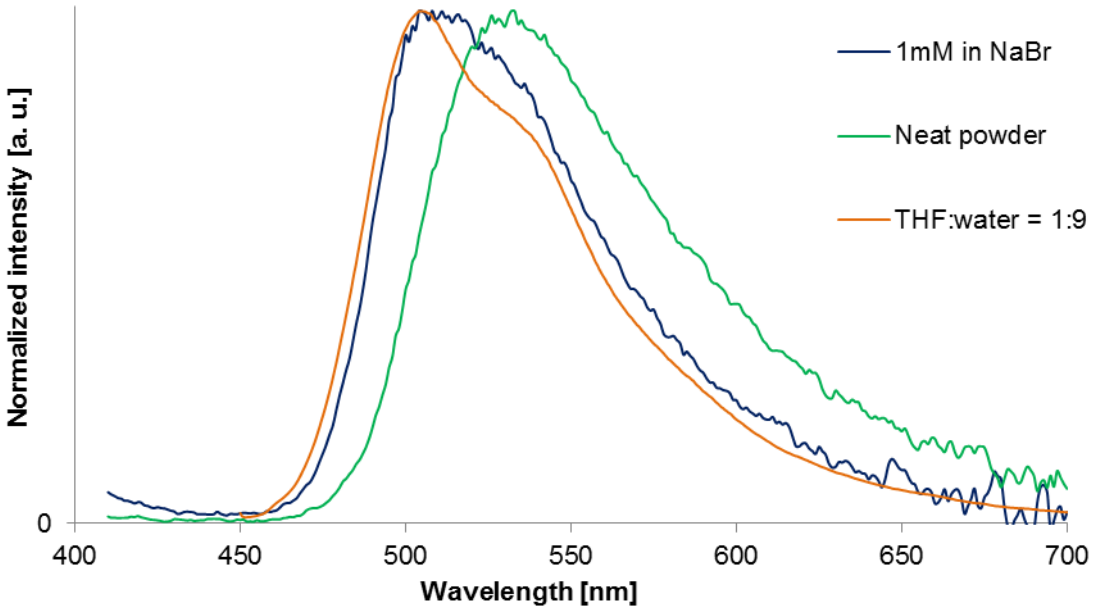

Fig. S58. Fluorescence spectra of **2,6-BPA** in the solid state (the excitation wavelength corresponds to the maxima of diffused-reflectance spectra observed from the dispersed state in NaBr).

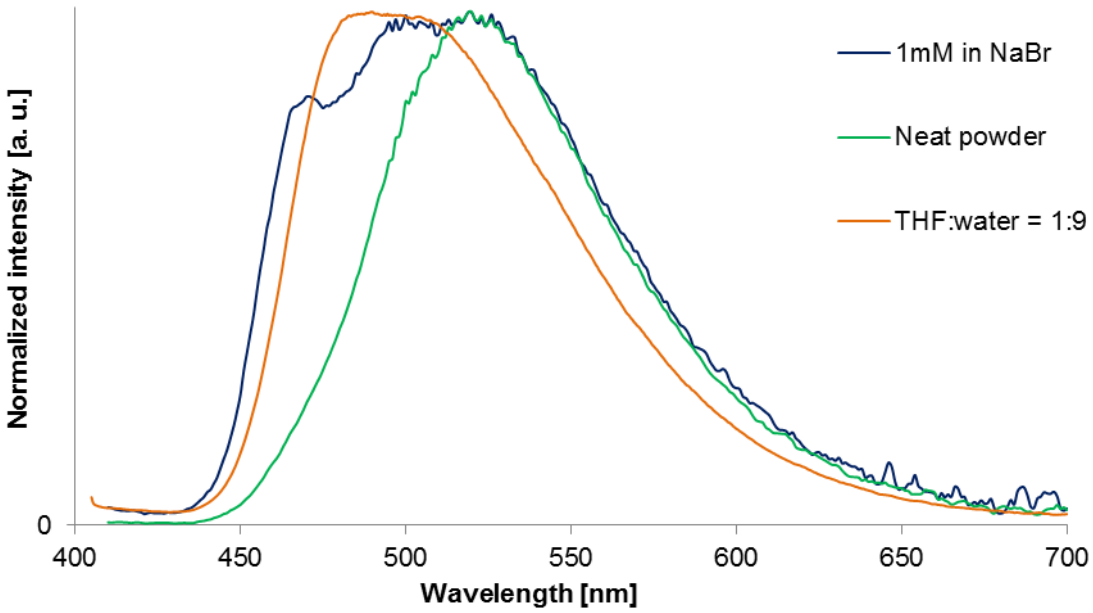

Fig. S59. Fluorescence spectra of **9-PA** in the solid state (the excitation wavelength corresponds to the maxima of diffused-reflectance spectra observed from the dispersed state in NaBr).

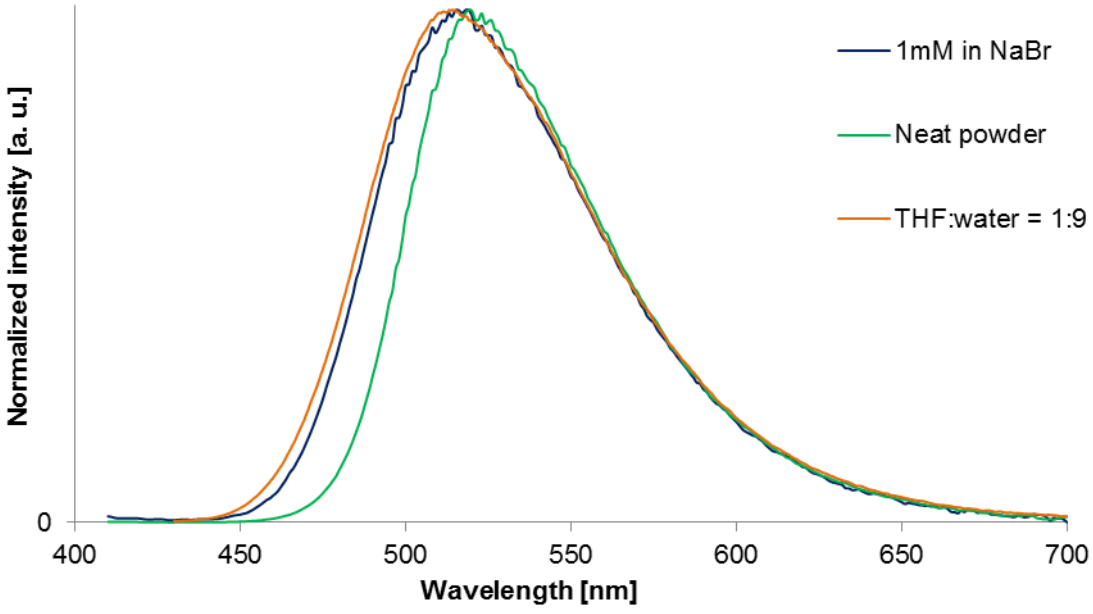

Fig. S60. Fluorescence spectra of **9,10-BPA** in the solid state (the excitation wavelength corresponds to the maxima of diffused-reflectance spectra observed from the dispersed state in NaBr).

S5. Crystallographic information

9-Piperidylanthracene (9-PA)

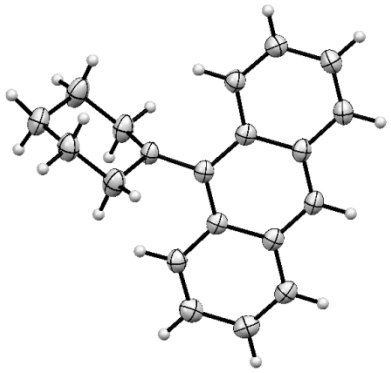

Fig. S61. ORTEP drawing of **9-PA** (thermal ellipsoids at 50% probability). Selected crystal parameters for **9-PA**: monoclinic, $P2_1/c$ (No. 14), a = 8.8386(6) Å, b = 21.570(2) Å, c = 7.7107(5) Å, β = 98.864(7) °, V = 1452.5(2) Å^3, Z = 4, R_1 = 0.0508, wR_2 = 0.1374. CCDC 1055226 contains the supplementary crystallographic data for this compound. These data can be obtained free of charge from The Cambridge Crystallographic Data Centre *via* www.ccdc.cam.ac.uk/data_request/cif.

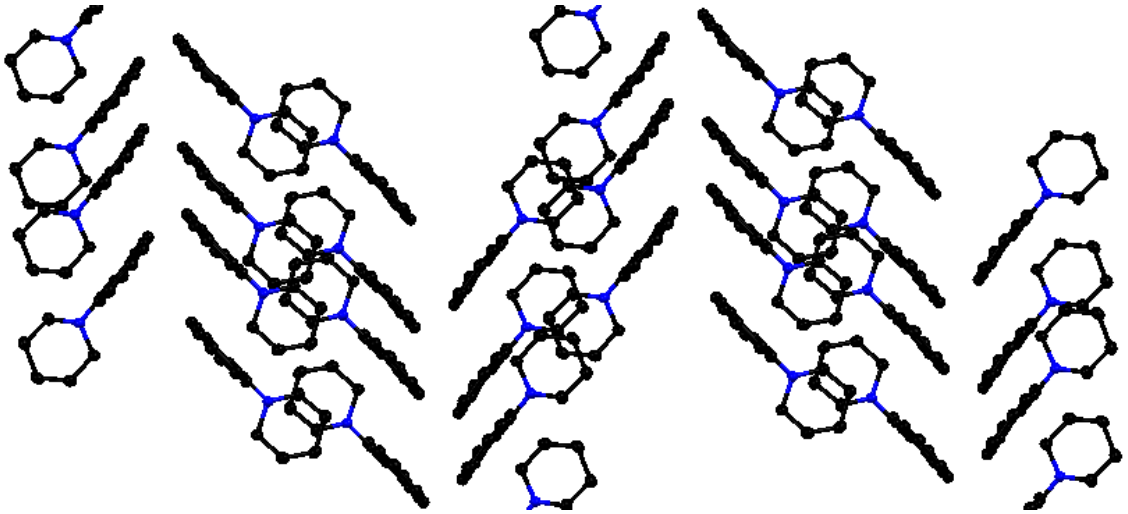

Fig. S62. Crystal packing of **9-PA** (hydrogen atoms omitted for clarity. Each ball represents the van der Waals radius of an atom. Colour code: blue – nitrogen; black – carbon).

9,10-Bis(piperidyl)anthracene (9,10-BPA)

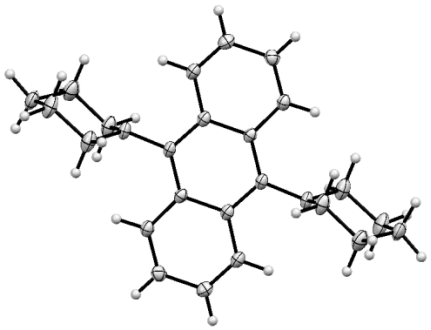

Fig. S63. ORTEP drawing of **9,10-BPA** (thermal ellipsoids at 50% probability). Selected crystal parameters for of **9,10-BPA**: triclinic, *P*-1 (No. 2), a = 7.388(2) Å, b = 7.625(2) Å, c = 9.047(3) Å, α = 101.595(6) °, β = 103.106(5) °, γ = 99.662(4) °, V = 473.9(3) Å^3, Z = 1, R_1 = 0.0802, wR_2 = 0.2243. CCDC 1055229 contains the supplementary crystallographic data for this compound. These data can be obtained free of charge from The Cambridge Crystallographic Data Centre *via* www.ccdc.cam.ac.uk/data_request/cif.

1,4-Bis(piperidyl)anthracene (1,4-BPA)

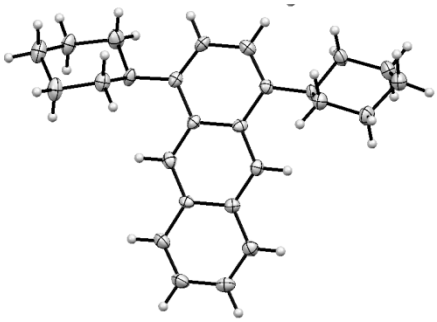

Fig. S64. ORTEP drawing of **1,4-BPA** (thermal ellipsoids at 50% probability). Selected crystal paramters for **1,4-BPA**: monoclinic, $P2_1/n$ (No. 14), a = 18.041(5) Å, b = 10.854(3) Å, c = 29.573(8) Å, β = 90.12(2) °, V = 5791.(3) Å^3, Z = 12, R_1 = 0.0531, wR_2 = 0.0863. CCDC 1055227 contains the supplementary crystallographic data for this compound. These data can be obtained free of charge from The Cambridge Crystallographic Data Centre *via* www.ccdc.cam.ac.uk/data_request/cif.

1,5-Bis(piperidyl)anthracene (1,5-BPA)

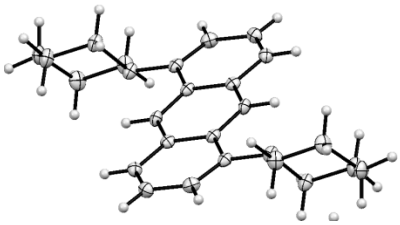

Fig. S65. ORTEP drawing of **1,5-BPA** (thermal ellipsoids at 50% probability). Selected crystal parameters for **1,5-BPA**: triclinic, *P*-1 (No. 2), a = 9.7682(10) Å, b = 10.058(2) Å, c = 10.3707(11) Å, α = 85.751(9) º, β = 66.290(7) °, γ = 83.253(9) º, V = 926.1(2) Å^3, Z = 2, R_1 = 0.0839, wR_2 = 0.2455. CCDC 1055228 contains the supplementary crystallographic data for this compund. These data can be obtained free of charge from The Cambridge Crystallographic Data Centre *via* www.ccdc.cam.ac.uk/data_request/cif.

S6. Computational calculations

The ground-state and excited-state equilibrium structures of 1,4-bis(piperidyl)anthracene (**1,4-BPA**) and 1,5-bis(piperidyl)anthracene (**1,5-BPA**) were fully optimized by self-consistent field calculations using ωB97X-D as the hybrid density functional and 6-311G(d,p)[2] as basis sets. Hybrid functionals of the ωB97-family can address non-local exchange correlation and especially ωB97X-D takes dispersion effects into consideration[3]. Therefore ωB97X-D is suitable for the calculation of molecules with severe steric repulsions in the excited states. The analytical frequencies were obtained for ground-state structures to ensure that a local energy minimum has been located. Excited-state equilibrium structures were optimized for first-singlet excited states. All calculations were performed using the Gaussian 09 program package.[4]

(1) Optimized geometries

Table S3. Atom coordinates and absolute energy levels for the ground state of **1,4-BPA** obtained from theoretical calculations.

1,4-BPA (Ground): E(RωB97X-D) = -1040.854657 hartree				
Center number	Atomic number	Coordinate (Angstroms)		
		X	Y	Z
1	6	2.542162	-0.16914	0.714237
2	6	2.542162	-0.16914	-0.71424
3	6	1.322779	-0.16652	-1.39216
4	6	0.106012	-0.13391	-0.71632
5	6	0.106012	-0.13391	0.716324
6	6	1.322779	-0.16652	1.392164
7	6	3.793819	-0.19635	1.401182
8	6	4.96681	-0.2163	0.711919
9	6	4.96681	-0.2163	-0.71192
10	6	3.793819	-0.19635	-1.40118
11	6	-1.15254	-0.17012	-1.42746
12	6	-2.30636	-0.2869	-0.71153
13	6	-2.30636	-0.2869	0.711529
14	6	-1.15254	-0.17012	1.427456
15	7	-1.11278	-0.11171	2.841933
16	7	-1.11278	-0.11171	-2.84193
17	6	-0.83982	1.22796	3.369382
18	6	-0.44338	1.155586	4.839253
19	6	-1.52108	0.441983	5.654867
20	6	-1.85473	-0.91123	5.027505

21	6	-2.20908	-0.75301	3.551602
22	6	-2.20908	-0.75301	-3.5516
23	6	-1.85473	-0.91123	-5.02751
24	6	-1.52108	0.441983	-5.65487
25	6	-0.44338	1.155586	-4.83925
26	6	-0.83982	1.22796	-3.36938
27	1	1.314469	-0.22726	-2.47435
28	1	1.314469	-0.22726	2.474347
29	1	3.789548	-0.1989	2.486349
30	1	5.911462	-0.23404	1.243658
31	1	5.911462	-0.23404	-1.24366
32	1	3.789548	-0.1989	-2.48635
33	1	-3.26017	-0.33902	-1.22259
34	1	-3.26017	-0.33902	1.222592
35	1	-0.04382	1.685082	2.779712
36	1	-1.73509	1.867119	3.256179
37	1	0.503947	0.610741	4.922052
38	1	-0.27455	2.166658	5.221377
39	1	-1.20108	0.317284	6.693048
40	1	-2.42623	1.062572	5.67277
41	1	-0.99109	-1.57974	5.108485
42	1	-2.68938	-1.38472	5.552979
43	1	-2.39109	-1.7286	3.095359
44	1	-3.14506	-0.16759	3.470893
45	1	-2.39109	-1.7286	-3.09536
46	1	-3.14506	-0.16759	-3.47089
47	1	-0.99109	-1.57974	-5.10849
48	1	-2.68938	-1.38472	-5.55298
49	1	-1.20108	0.317284	-6.69305
50	1	-2.42623	1.062572	-5.67277
51	1	0.503947	0.610741	-4.92205
52	1	-0.27455	2.166658	-5.22138
53	1	-0.04382	1.685082	-2.77971
54	1	-1.73509	1.867119	-3.25618

Table S4. Atom coordinates and absolute energy levels for the excited state of 1,4-bis(piperidyl)anthracene (**1,4-BPA**) obtained from theoretical calculations.

1,4-BPA (Excited): *E*(TD-*ω*B97X-D) = -1040.746305 hartree				
Center number	Atomic number	Coordinate (Angstroms)		
		X	Y	Z
1	6	2.495913	0.187399	-0.71411
2	6	2.495913	0.187399	0.714111
3	6	1.24712	0.180486	1.395538
4	6	0.025976	0.106341	0.71626
5	6	0.025976	0.106341	-0.71626
6	6	1.24712	0.180486	-1.39554
7	6	3.725793	0.226032	-1.39057
8	6	4.928219	0.260571	-0.69674

9	6	4.928219	0.260571	0.696741
10	6	3.725793	0.226032	1.390567
11	6	-1.22887	0.138199	1.409052
12	6	-2.426	0.366188	0.685967
13	6	-2.426	0.366188	-0.68597
14	6	-1.22887	0.138199	-1.40905
15	7	-1.27079	-0.03293	-2.77598
16	7	-1.27079	-0.03293	2.775983
17	6	-0.6621	-1.22306	-3.37669
18	6	-0.14256	-0.9309	-4.77829
19	6	-1.25738	-0.35804	-5.65263
20	6	-1.90326	0.845908	-4.96908
21	6	-2.37625	0.500655	-3.5567
22	6	-2.37625	0.500655	3.556698
23	6	-1.90326	0.845908	4.969077
24	6	-1.25738	-0.35804	5.652626
25	6	-0.14256	-0.9309	4.778286
26	6	-0.6621	-1.22306	3.376687
27	1	1.255486	0.310327	2.470217
28	1	1.255486	0.310327	-2.47022
29	1	3.724858	0.234512	-2.47648
30	1	5.865695	0.292904	-1.24083
31	1	5.865695	0.292904	1.240826
32	1	3.724858	0.234512	2.476481
33	1	-3.37032	0.415736	1.211989
34	1	-3.37032	0.415736	-1.21199
35	1	0.130947	-1.58286	-2.72565
36	1	-1.43439	-2.00864	-3.43043
37	1	0.684414	-0.21577	-4.71127
38	1	0.256701	-1.85193	-5.2118
39	1	-0.87161	-0.07597	-6.63571
40	1	-2.01828	-1.13146	-5.81857
41	1	-1.17809	1.66351	-4.90039
42	1	-2.75578	1.210694	-5.54936
43	1	-2.75125	1.399822	-3.06752
44	1	-3.20248	-0.22904	-3.61147
45	1	-2.75125	1.399822	3.067519
46	1	-3.20248	-0.22904	3.611474
47	1	-1.17809	1.66351	4.900387
48	1	-2.75578	1.210694	5.549358
49	1	-0.87161	-0.07597	6.635705
50	1	-2.01828	-1.13146	5.818569
51	1	0.684414	-0.21577	4.711265
52	1	0.256701	-1.85193	5.211803
53	1	0.130947	-1.58286	2.725654
54	1	-1.43439	-2.00864	3.430429

Table S5. Atom coordinates and absolute energy levels for the ground state of 1,5-bis(piperidyl)anthracene (**1,5-BPA**) obtained from theoretical calculations.

1,5-BPA (Ground): E(RωB97X-D) = -1040.855008 hartree				
Center number	Atomic number	Coordinate (Angstroms)		
		X	Y	Z
1	6	-1.34437	-0.19086	-0.37847
2	6	-0.51215	-1.31755	-0.08835
3	6	0.806801	-1.09378	0.299266
4	6	1.344367	0.190856	0.378472
5	6	0.512147	1.317554	0.088349
6	6	-0.8068	1.09378	-0.29927
7	6	-2.71704	-0.40494	-0.71175
8	6	-3.22694	-1.66303	-0.73477
9	6	-2.39883	-2.79168	-0.48152
10	6	-1.07154	-2.64685	-0.18762
11	6	2.717041	0.404943	0.711753
12	6	3.22694	1.663033	0.734766
13	6	2.398829	2.791677	0.481516
14	6	1.07154	2.646847	0.18762
15	7	0.206632	3.742393	-0.04231
16	7	-0.20663	-3.74239	0.042313
17	6	-0.70952	4.021025	1.067802
18	6	-1.84391	4.930376	0.610604
19	6	-1.29101	6.219973	0.00432
20	6	-0.26413	5.901009	-1.08204
21	6	0.815601	4.962515	-0.55074
22	6	-0.8156	-4.96252	0.550738
23	6	0.264132	-5.90101	1.082038
24	6	1.291006	-6.21997	-0.00432
25	6	1.84391	-4.93038	-0.6106
26	6	0.709519	-4.02103	-1.0678
27	1	1.428172	-1.9428	0.559475
28	1	-1.42817	1.942798	-0.55948
29	1	-3.34244	0.455369	-0.92449
30	1	-4.27288	-1.82434	-0.97098
31	1	-2.83359	-3.78146	-0.54984
32	1	3.342437	-0.45537	0.924489
33	1	4.272877	1.824339	0.970982
34	1	2.833591	3.78146	0.549839
35	1	-1.10264	3.078345	1.450262
36	1	-0.15834	4.502076	1.896741
37	1	-2.44298	4.397645	-0.13668
38	1	-2.49834	5.151064	1.458978
39	1	-2.1	6.83532	-0.3989
40	1	-0.80688	6.808071	0.794542
41	1	-0.76022	5.416222	-1.92947
42	1	0.202272	6.818503	-1.45297
43	1	1.513834	4.694196	-1.34658

44	1	1.391006	5.488772	0.234568
45	1	-1.51383	-4.6942	1.346583
46	1	-1.39101	-5.48877	-0.23457
47	1	0.76022	-5.41622	1.929469
48	1	-0.20227	-6.8185	1.452968
49	1	2.099995	-6.83532	0.398903
50	1	0.806883	-6.80807	-0.79454
51	1	2.442982	-4.39765	0.136677
52	1	2.498339	-5.15106	-1.45898
53	1	1.102638	-3.07835	-1.45026
54	1	0.158341	-4.50208	-1.89674

Table S6. Atom coordinates and absolute energy levels for the excited state of 1,5-bis(piperidyl)anthracene (**1,5-BPA**) obtained from theoretical calculations

1,5-BPA (Excited): *E*(TD-*ω*B97X-D) = -1040.738666 hartree				
Center number	Atomic number	Coordinate (Angstroms)		
		X	Y	Z
1	6	-1.36754	-0.18951	-0.35188
2	6	-0.54205	-1.32899	-0.05887
3	6	0.789123	-1.10428	0.321913
4	6	1.367535	0.189505	0.351882
5	6	0.542054	1.328994	0.058874
6	6	-0.78912	1.104277	-0.32191
7	6	-2.72338	-0.38183	-0.62543
8	6	-3.28706	-1.6641	-0.61508
9	6	-2.49881	-2.77184	-0.37624
10	6	-1.11349	-2.62805	-0.14112
11	6	2.723382	0.38183	0.625434
12	6	3.287057	1.6641	0.615078
13	6	2.498807	2.771835	0.376236
14	6	1.11349	2.628047	0.141121
15	7	0.282695	3.745387	0.002425
16	7	-0.2827	-3.74539	-0.00243
17	6	-0.72676	3.954305	1.044754
18	6	-1.86632	4.822509	0.526716
19	6	-1.32855	6.148243	-0.01177
20	6	-0.22009	5.899093	-1.03392
21	6	0.867633	4.994145	-0.45787
22	6	-0.86763	-4.99415	0.457873
23	6	0.220091	-5.89909	1.033924
24	6	1.328553	-6.14824	0.011769
25	6	1.866317	-4.82251	-0.52672
26	6	0.726763	-3.95431	-1.04475
27	1	1.397635	-1.94588	0.632356
28	1	-1.39764	1.945878	-0.63236
29	1	-3.34832	0.481853	-0.82736
30	1	-4.34279	-1.78964	-0.82642

31	1	-2.93524	-3.7615	-0.42287
32	1	3.348318	-0.48185	0.827363
33	1	4.342791	1.789637	0.826424
34	1	2.935241	3.761495	0.422866
35	1	-1.09585	2.986388	1.381025
36	1	-0.25347	4.447223	1.912644
37	1	-2.38856	4.282084	-0.27094
38	1	-2.58632	4.995198	1.331904
39	1	-2.13329	6.740413	-0.45593
40	1	-0.92384	6.735598	0.822467
41	1	-0.63912	5.41515	-1.92246
42	1	0.229559	6.843716	-1.35408
43	1	1.611476	4.769409	-1.22433
44	1	1.381577	5.524302	0.365277
45	1	-1.61148	-4.76941	1.224331
46	1	-1.38158	-5.5243	-0.36528
47	1	0.63912	-5.41515	1.922456
48	1	-0.22956	-6.84372	1.354076
49	1	2.133288	-6.74041	0.455932
50	1	0.923837	-6.7356	-0.82247
51	1	2.388556	-4.28208	0.270938
52	1	2.586322	-4.9952	-1.3319
53	1	1.095852	-2.98639	-1.38103
54	1	0.253466	-4.44722	-1.91264

(2) Frontier orbitals

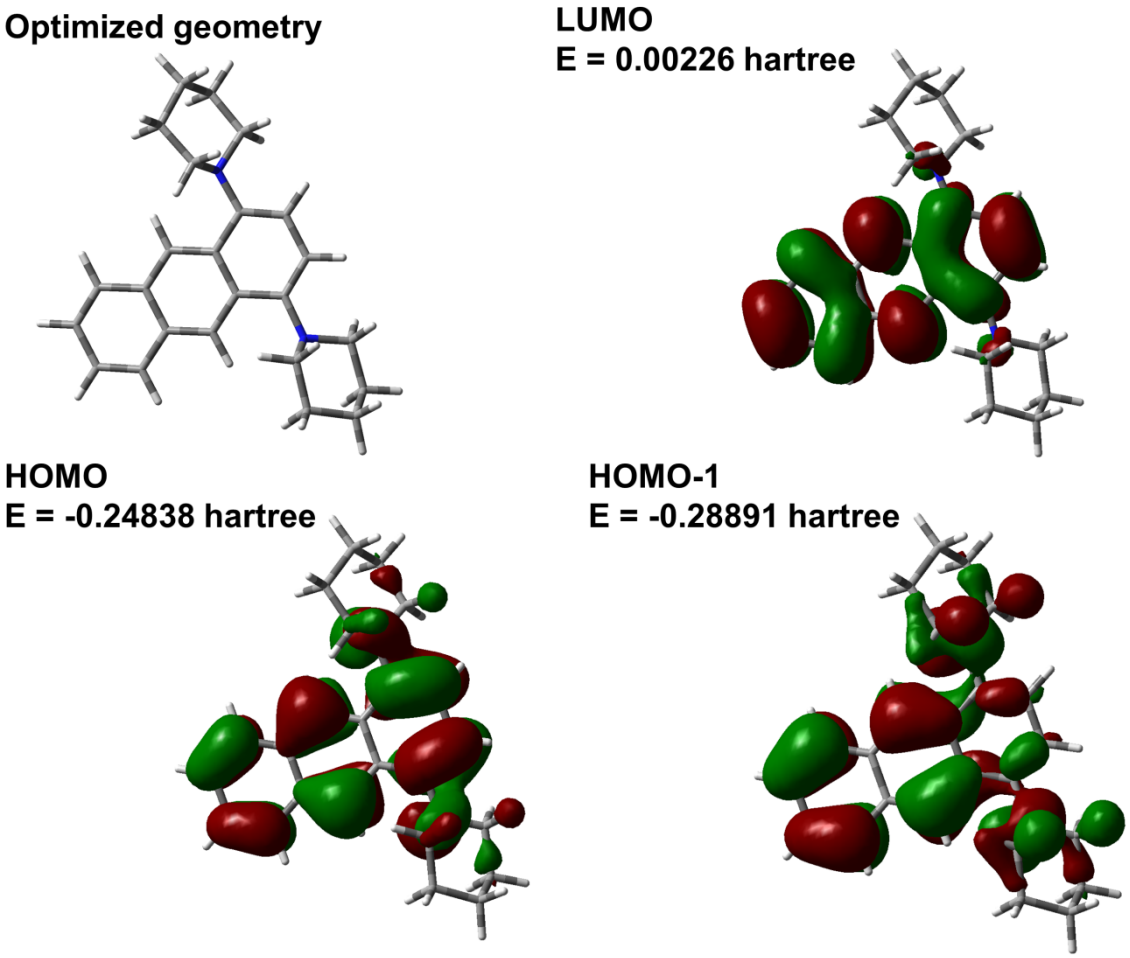

Fig. S66. Frontier orbitals for the ground state of **1,4-BPA**.

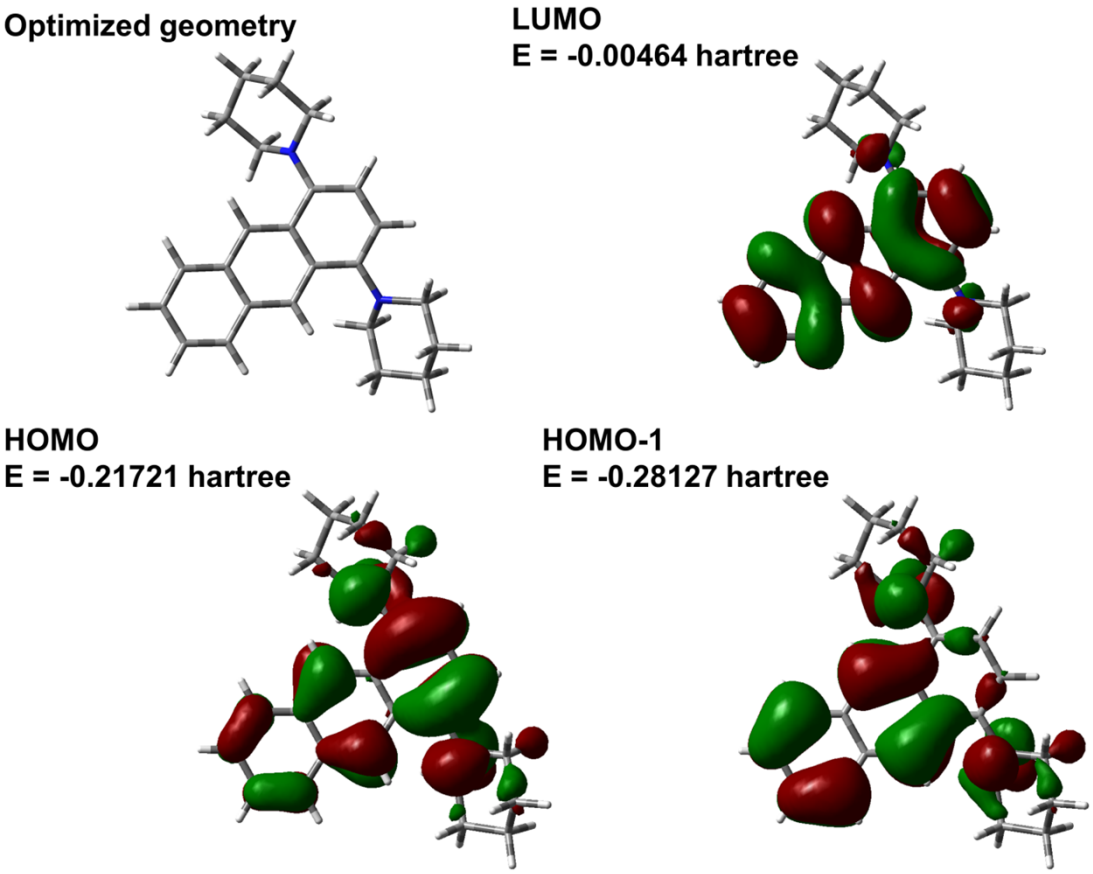

Fig. S67. Frontier orbitals for the excited state of **1,4-BPA**.

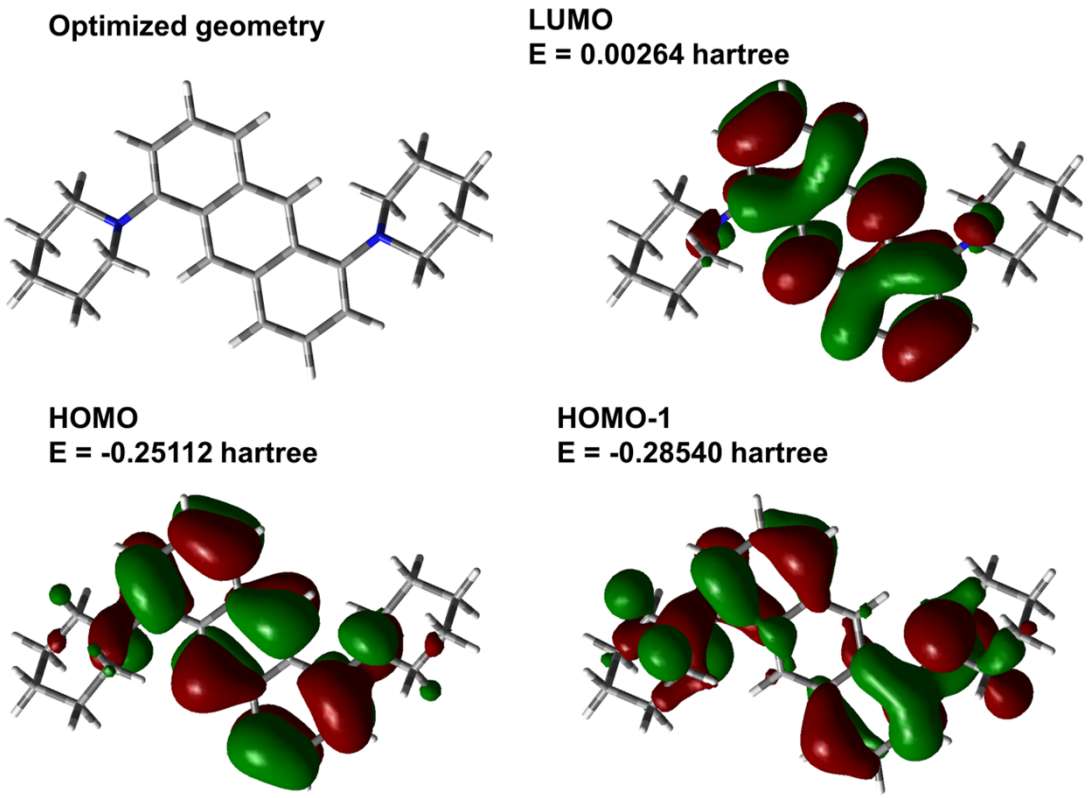

Fig. S68. Frontier orbitals for the ground state of **1,5-BPA**.

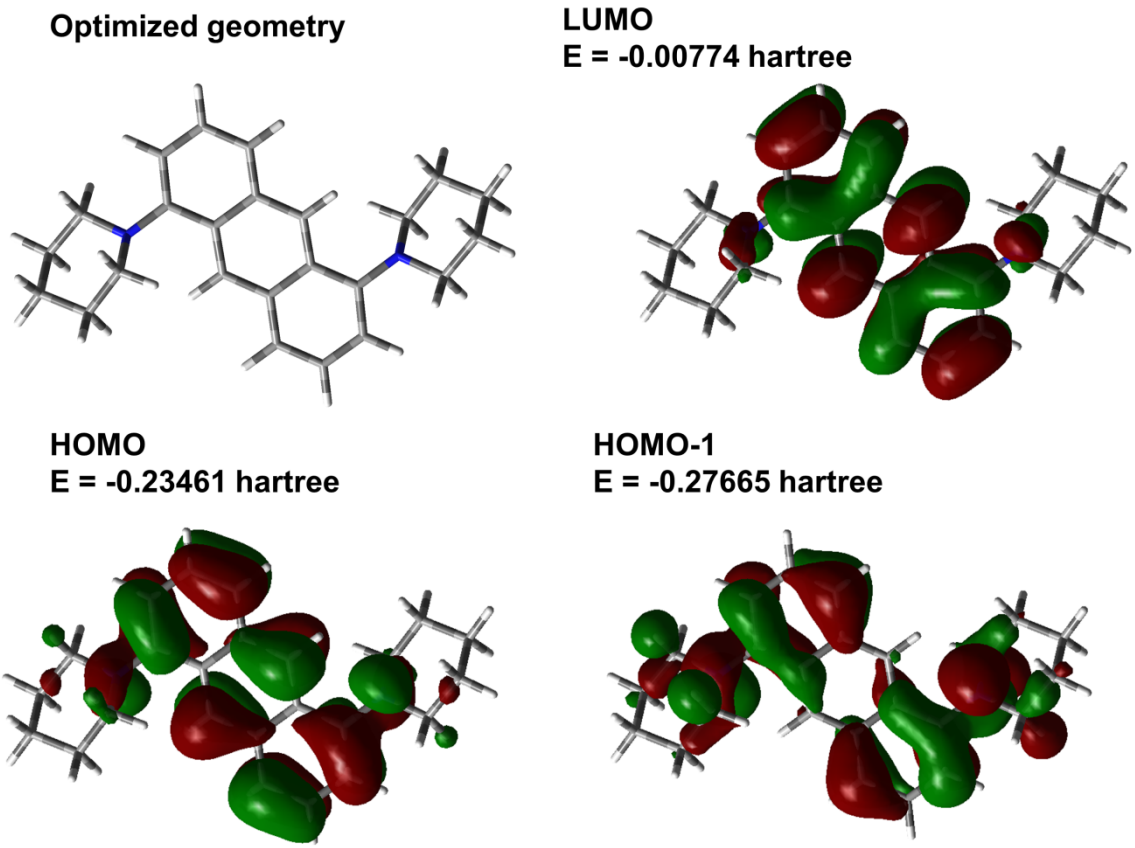

Fig. S69. Frontier orbitals for the excited state of **1,5-BPA**.

(3) Optical transitions

Table S7. Excitation energies, oscillator strengths, main transition orbitals, and associated contributions calculated for the ground and excited state of **1,4-BPA** (ωB97X-D/6-311G(d,p)).

Entry	State	Excitation energy [eV]	Transition wavelength [nm]	Oscillator strength	Main transition orbital	Contribution
1,4-BPA (Ground state)	T_1	1.83	677	0	HOMO-4→LUMO+2	0.03
					HOMO-3→LUMO+1	0.02
					HOMO-1→LUMO	0.10
					HOMO-1→LUMO+2	0.02
					HOMO→LUMO	0.79
					HOMO←LUMO	0.04
	T_2	3.06	405	0	HOMO-5→LUMO+2	0.02
					HOMO-4→LUMO	0.10
					HOMO-1→LUMO	0.54
					HOMO→LUMO	0.04
					HOMO→LUMO+2	0.29
	S_1	3.41	364	0.17	HOMO→LUMO	1.00
	T_3	3.66	339	0	HOMO-3→LUMO	0.07
					HOMO-1→LUMO+1	0.04
					HOMO→LUMO+1	0.89
	T_4	3.85	322	0	HOMO-3→LUMO	0.41
					HOMO-2→LUMO	0.52
					HOMO→LUMO+1	0.06
	S_2	4.06	305	0.0055	HOMO-3→LUMO	0.18
					HOMO-2→LUMO	0.25
					HOMO-1→LUMO+1	0.03
					HOMO→LUMO+1	0.53
1,4-BPA (Excited state)	T_1	0.95	1305	0	HOMO-3→LUMO+1	0.02
					HOMO-1→LUMO	0.08
					HOMO→LUMO	0.74
					HOMO→LUMO+2	0.04
					HOMO-1←LUMO	0.02
					HOMO←LUMO	0.10
	S_1	2.45	506	0.1477	HOMO→LUMO	1.00
	T_2	2.49	498	0	HOMO-4→LUMO	0.02
					HOMO-1→LUMO	0.71
					HOMO→LUMO	0.03
					HOMO→LUMO+2	0.21
					HOMO→LUMO+3	0.03
	T_3	3.09	402	0	HOMO→LUMO+1	0.94
					HOMO→LUMO+8	0.06
	S_2	3.65	340	0.0756	HOMO-3→LUMO	0.17
					HOMO-2→LUMO	0.05
					HOMO→LUMO+1	0.78
	T_4	3.75	331	0	HOMO-3→LUMO	0.70
					HOMO-2→LUMO	0.30

Table S8. Excitation energies, oscillator strengths, main transition orbitals, and associated contributions calculated for the ground and excited state of **1,5-BPA**

(ωB97X-D/6-311G(d,p)).

Entry	State	Excitation energy [eV]	Transition wavelength [nm]	Oscillator strength	Main transition orbital	Contribution
1,5-BPA (Ground state)	T_1	1.84	675	0	HOMO-4→LUMO+2	0.02
					HOMO-3→LUMO+1	0.02
					HOMO-2→LUMO	0.02
					HOMO-1→LUMO+2	0.04
					HOMO→LUMO	0.85
					HOMO←LUMO	0.05
	T_2	3.09	401	0	HOMO-5→LUMO+2	0.02
					HOMO-4→LUMO	0.11
					HOMO-1→LUMO	0.53
					HOMO→LUMO+2	0.34
	S_1	3.49	355	0.1986	HOMO→LUMO	1.00
	T_3	3.69	336	0	HOMO-3→LUMO	0.08
					HOMO→LUMO+1	0.92
	T_4	3.83	324	0	HOMO-5→LUMO	0.04
					HOMO-3→LUMO	0.11
					HOMO-2→LUMO	0.76
					HOMO-1→LUMO+2	0.02
					HOMO→LUMO+1	0.04
					HOMO→LUMO+3	0.03
	T_5	3.95	314	0	HOMO-5→LUMO	0.13
					HOMO-3→LUMO	0.54
					HOMO-1→LUMO+2	0.14
					HOMO→LUMO+1	0.06
					HOMO→LUMO+3	0.13
1,5-BPA (Excited state)	T_1	1.06	1169	0	HOMO-3→LUMO+1	0.02
					HOMO-2→LUMO	0.03
					HOMO-1→LUMO+2	0.03
					HOMO→LUMO	0.80
					HOMO←LUMO	0.12
	T_2	2.63	472	0	HOMO-4→LUMO	0.07
					HOMO-1→LUMO	0.62
					HOMO→LUMO+2	0.31
	S_1	2.85	435	0.2124	HOMO→LUMO	1.00
	T_3	3.39	365	0	HOMO-2→LUMO	0.06
					HOMO→LUMO+1	0.94
	T_4	3.53	352	0	HOMO-5→LUMO	0.12
					HOMO-2→LUMO	0.59
					HOMO-1→LUMO+2	0.10
					HOMO→LUMO+1	0.09
					HOMO→LUMO+3	0.10
	T_5	3.73	332	0	HOMO-6→LUMO+2	0.02
					HOMO-5→LUMO	0.02
					HOMO-3→LUMO	0.79
					HOMO-2→LUMO	0.08
					HOMO-1→LUMO+2	0.05
					HOMO→LUMO+3	0.04

S7. References

(1) A. Sillen and Y. Engelborghs, *Photochem. Photobiol.,* 1998, **67**, 475-486.

(2) (*a*) J.-D. Chai and M. Head-Gordon, *Phys. Chem. Chem. Phys*., 2008, **10**, 6615-6620; (*b*) R. Ditchfield, W. J. Hehre and J. A. Pople, *J. Chem. Phys*., 1971, **54**, 724-728; (*c*) W. J. Hehre, R. Ditchfield and J. A. Pople, *J. Chem. Phys*., 1972, **56**, 2257-2261; (*d*) P. C. Hariharan and J. A. Pople, *Theor. Chem. Acc*., 1973, **28**, 213-222; (*e*) P. C. Hariharan and J. A. Pople, *Mol. Phys.*, 1974, **27**, 209-214.

(3) (*a*) N. Mardirossian, J. A. Parkhill and M. Head-Gordon, *Phys. Chem. Chem. Phys.*, 2011, **13**, 19325-19337; (*b*) D. Jacquemin, E. A. Perpète, I. Ciofini and C. Adamo, *Theor. Chem. Acc.*, 2011, **128**, 127-136.

(4) Gaussian 09, Revision C.01, M. J. Frisch, G. W. Trucks, H. B. Schlegel, G. E. Scuseria, M. A. Robb, J. R. Cheeseman, G. Scalmani, V. Barone, B. Mennucci, G. A. Petersson, H. Nakatsuji, M. Caricato, X. Li, H. P. Hratchian, A. F. Izmaylov, J. Bloino, G. Zheng, J. L. Sonnenberg, M. Hada, M. Ehara, K. Toyota, R. Fukuda, J. Hasegawa, M. Ishida, T. Nakajima, Y. Honda, O. Kitao, H. Nakai, Vreven, T.; Montgomery, J. A.; J. E. Peralta, Jr., F. Ogliaro, M. Bearpark, J. J. Heyd, E. Brothers, K. N. Kudin, V. N. Staroverov, R. Kobayashi, J. Normand, K. Raghavachari, A. Rendell, J. C. Burant, S. S. Iyengar, J. Tomasi, M. Cossi, N. Rega, J. M. Millam, M. Klene, J. E. Knox, J. B. Cross, V. Bakken, C. Adamo, J. Jaramillo, R. Gomperts, R. E. Stratmann, O. Yazyev, A. J. Austin, R. Cammi, C. Pomelli, J. W. Ochterski, R. L. Martin, K. Morokuma, V. G. Zakrzewski, G. A. Voth, P. Salvador, J. J. Dannenberg, S. Dapprich, A. D. Daniels, Ö. Farkas, J. B. Foresman, J. V. Ortiz, J. Cioslowski, D. J. Fox, Gaussian, Inc., Wallingford CT, 2010.